DEVELOPING A GLOBAL VEGETATION DYNAMICS MODEL: RESULTS OF AN IIASA SUMMER WORKSHOP

I. Colin Prentice, Robert S. Webb, Mikhail T. Ter-Mikhaelian, Allen M. Solomon, Thomas M. Smith, Sergei E. Pitovranov, Nedialko T. Nikolov, Alexander A. Minin, Rik Leemans, Sandra Lavorel, Mikhail D. Korzukhin, Janos P. Hrabovszky, Harry O. Helmisaari, Sandy P. Harrison, William R. Emanuel, and Gordon B. Bonan

RR–89–7
August 1989

INTERNATIONAL INSTITUTE FOR APPLIED SYSTEMS ANALYSIS
Laxenburg, Austria

International Standard Book Number 3-7045-0095-X

Research Reports, which record research conducted at IIASA, are independently reviewed before publication. However, the views and opinions they express are not necessarily those of the Institute or the National Member Organizations that support it.

Cover design by Martin Schobel

Printed by Novographic, Vienna, Austria

Foreword

IIASA's projects within the Environment Program are devoted to investigating the interaction of human development activities and the environment, particularly in terms of the sustainable development of the biosphere. The research is policy-oriented, interdisciplinary, international in scope and heavily dependent on collaboration with a network of research scientists and institutes in many countries. The importance of IIASA's Environment Program stems from the fact that the many components of the planetary life-support systems are being threatened by increasing human activity, and that these problems are not susceptible to solution by singular governments or even, international agencies. Instead, resolution of the difficulties will demand concerted and cooperative actions by many governments and agencies, based on valid understanding of the earth's environmental systems. Establishment of a basis for international cooperation, and production of accurate global environmental perceptions are both hallmarks of IIASA's Environment Program.

Foremost among the global environmental issues of concern are those involving declining amounts of stratospheric ozone, increasing atmospheric concentrations of greenhouse gases, and changing climate. Problem solutions will only become apparent after collection and analysis of pertinent data, testing of relevant hypotheses, genesis of mitigation strategies, and investigation of the efficacy of the strategies which are developed. All of these activities can support development of, or be supported by, the appropriate mathematical models of the biosphere. Therefore, the Biosphere Dynamics Project has focused on the creation of models which can describe the vegetation dynamics portion of the biosphere. The models are being designed to define the biotic and ecological results of measures suggested to slow or stop increases in greenhouse gases. The models must be capable of documenting whether, and if so, by how much, vegetational communities would benefit from mitigation actions, as well as describing how the terrestrial biosphere will respond in its role as carbon source and sink.

The following report provides the initial substantive description of such a global vegetation model which was generated through the interactions of eighteen graduate students, visitors and resident scholars at IIASA during the summer of 1988. Independent but related activities in modifying detailed dynamic

models of boreal forest systems are described here as well. This particular summer workshop, in attracting a critical mass of highly qualified scientists to IIASA for several months, has proven to be extremely advantageous in attacking difficult, complex, and interdisciplinary scientific problems. As a result, the summer-long workshop is being repeated in 1989 with a related but different set of research problems and scientists. We hope that these summer workshops can become a commonly applied approach to scientific problem solving at IIASA during the coming years. In the meantime, the following discussion of results from the 1988 prototype workshop illustrates a highly productive and satisfying endeavor.

BO R. DÖÖS
Program Leader
Environment Program

Preface

During summer of 1987, a series of discussions among A.M. Solomon, H.H. Shugart, W.C. Clark, R.E. Munn, and M.Ya. Antonovsky at IIASA led to plans for a study of global vegetation change. The research was subsequently funded by a grant from the A.P. Sloan Foundation in fall 1987, and began in earnest in spring 1988. The work was to be aimed specifically at the International Geosphere-Biosphere Programme (IGBP), sponsored by the International Council of Scientific Unions (ICSU), of which IIASA is a member. IGBP aims to understand global environmental changes which result from human activity and which may threaten life. Predictive models of the Geosphere-Biosphere System are a primary means of studying the nature, effects and controls of environmental change, and form a key part of the planned IGBP strategy. Such models are being devised to examine the likely sensitivities and vulnerabilities of biosphere functioning, and to define necessary monitoring systems. The IIASA study on Global Vegetation Change represents a *stalking horse* for the models, that is, an exercise to provide concrete guidance in formulating the working plans of IGBP.

Our objective was to develop a mathematical model of global vegetation, including agriculture, as defined by the forces which control and change vegetation. The model is expected to illustrate the geographical consequences to vegetation structure and function of changing climate and land use, based on plant responses to environmental variables. The completed model will also be used for examining international environmental policy responses to global change, as well as for studying the validity of IIASA's approaches to environmental policy development.

The project got under way with a meeting of 65 scientists from 20 nations held at IIASA in April 1988. The meeting brought together the principal and potential contributors to the project. Among those present were IGBP leaders who will observe, advise on, and assimilate from the project. The meeting was called to define the function of the global vegetation modeling system, how it will be used, and by whom; the salient vegetation responses to climate and soils which must be incorporated; the land use and soils effects and responses to be included; the geographic climate data sets and classifications available; the

modeling approaches most appropriate for the task; and the nature of the interfaces between the model and its prospective users.

The results of this planning meeting were used during a summer-long workshop at IIASA in 1988. The workshop aimed to develop a strategy to model global vegetation change. Eight ecologists and modelers and six graduate students spent much of the three summer months of 1988 at IIASA.

In addition to the visiting scientists, two Biosphere staff members and six graduate students in the IIASA Young Scientist's Summer Program (YSSP) worked within the group. The six students possessed strong biological and modeling backgrounds, and were drawn from as many different countries, providing a tremendous range of experiences and approaches to problem-solving. The result of the interactions among these 16 workers, plus the frequent, shorter-term visitors to the project, is reported below. With the exception of Colin Prentice, who coordinated this report, the authors are listed in reverse alphabetical order.

ALLEN M. SOLOMON
Project Leader
Biosphere Dynamics Project

Acknowledgments

We thank Mark Fulton, who helped design the population dynamics model; David Skole and Wolfgang Cramer, whose visits to the project helped define our approaches; Mikhail Antonovsky, Hank Shugart, William C. Clark, R.E. Ted Munn, and Victor Targulian for stimulating discussions and valuable ideas. Marilyn Brandl provided editorial assistance.

This research was supported by the A.P. Sloan Foundation, and the U.S. National Science Foundation through Grant INT87-06669 to the American Academy of Arts and Sciences, Cambridge, MA.

Contents

DEVELOPING A GLOBAL VEGETATION DYNAMICS MODEL: RESULTS OF AN IIASA SUMMER WORKSHOP

1. Introduction

Climate and the biosphere are broadly overlapping concepts. The biosphere is commonly taken to include not only the world's biota, but also soils, lakes, rivers, the surface layers of the ocean, and the lower atmosphere – the entire physical matrix that supports life (Vernadsky, 1945; Clark, 1986). The climate system includes ice sheets, oceans, and vegetation – all of which affect and are affected by the circulation and chemical composition of the atmosphere (Bolin, 1984). Both are part of a coupled global system characterized by processes operating on a very wide range of time scales.

The complexity of the global system, and the impossibility of controlled experiments, make quantitative, computer-intensive modeling essential. Atmospheric general circulation models (GCMs) are well developed. They describe the fast dynamics of the climate system – the response of circulation patterns to the boundary conditions imposed by solar radiation, atmospheric composition, and the instantaneous state of the land and water surfaces. But we also need to model slower components, including the response of the vegetation cover and surface hydrology to soil characteristics and longer-term values of atmospheric properties such as mean air temperature, precipitation, and potential evapotranspiration. The development of such a *slow* modeling framework is a necessary step towards a better understanding of the role played by the vegetation cover in the long-term dynamics of the biosphere and climate.

The interdependence of climate and life cannot be scrutinized from a narrow disciplinary perspective. For practical reasons, models of different components of the global system are developed separately; however, the appropriate division is not according to physical and biological boundaries. Organization according to characteristic response times can be more useful. Atmospheric models incorporate vegetation dynamics on short time scales (hours to months) according to the phenology of leaf area and stomatal aperture (Dickinson, 1984; Sellers *et al.*, 1986). In the longer term (years to centuries and millenia), vegetation composition and structure also change in response to changing climate

(Prentice 1986 and 1989). These changes may have far-reaching feedback effects on climate through regional changes in the hydrologic cycle and global changes in the carbon cycle (Solomon, 1986). We need global models with a lower time resolution, but with a longer time horizon than GCMs to model these longer-term interactions.

We call this type of longer-term model a (dynamic) global vegetation model (GVM). The emphasis on vegetation reflects its central role in mediating interactions between climate and earth systems, but such a model should not be confined to simulating vegetation processes. We envisage a model of the dynamics of the soil-plant-atmosphere system on time scales of 10–1000 years that includes all the critical ecosystem processes – physical, chemical, and biological – operating on this time scale.

This report describes the preliminary design for a global vegetation modeling scheme developed by the IIASA biosphere modeling workshop during summer 1988. This work is aimed at the eventual production of a model equivalent to general circulation models of the atmosphere. It will include two essential parts (see *Figure 1*): (1) a DYNAMIC stand simulator which works at the taxonomic resolution of plant functional types to provide temporal patterns of plant growth, mineral cycling, etc., and (2) a SPATIAL static model, composed of a coarse regional grid which will contain the constraints to plant growth (monthly temperatures, precipitation, and variables derived from these; character and variation in soil texture, water holding capacity and fertility; topographic diversity; solar insolation and latitude effects). The dynamic stand simulators (bottom of *Figure 1*) will be nested within each grid cell of the spatial static model (top of *Figure 1*). The coarse grid system will also serve as a close-ended exercise to define climate-dictated life zones, allowing the definition of potential life zones which could result from future climate changes. This latter exercise will include definitions of geographic boundaries of potential crop zones as well as vegetation life zones.

In Section 2 we begin by describing progress toward an independent model that will simulate forest responses to environmental change anywhere in the boreal zone. The core vegetation dynamics model used in this part of the work is a forest succession model (Shugart, 1984) that simulates interactions among individual trees through their effects on and responses to changes in the physical environment of a *circa* 1000 m^2 patch. Although it has no direct role in our global vegetation dynamics model, it may eventually provide an independent check on the validity of the coarse-scale global model, in that the boreal model contains much more detailed environmental processes, forces and responses than is possible on a global scale.

Forest succession models are powerful tools for regional studies, but they may be too detailed for simultaneous solution at a large number of locations. Section 3 describes the development of a more concise, computationally less demanding vegetation patch model. We also discuss the principles underlying the definition of plant functional types as basic taxonomic units in this model and the way in which different types respond to the external environment. Section 3 further examines the effects of the environment on the probability of natural disturbance. It suggests modeling the disturbance regime of a large

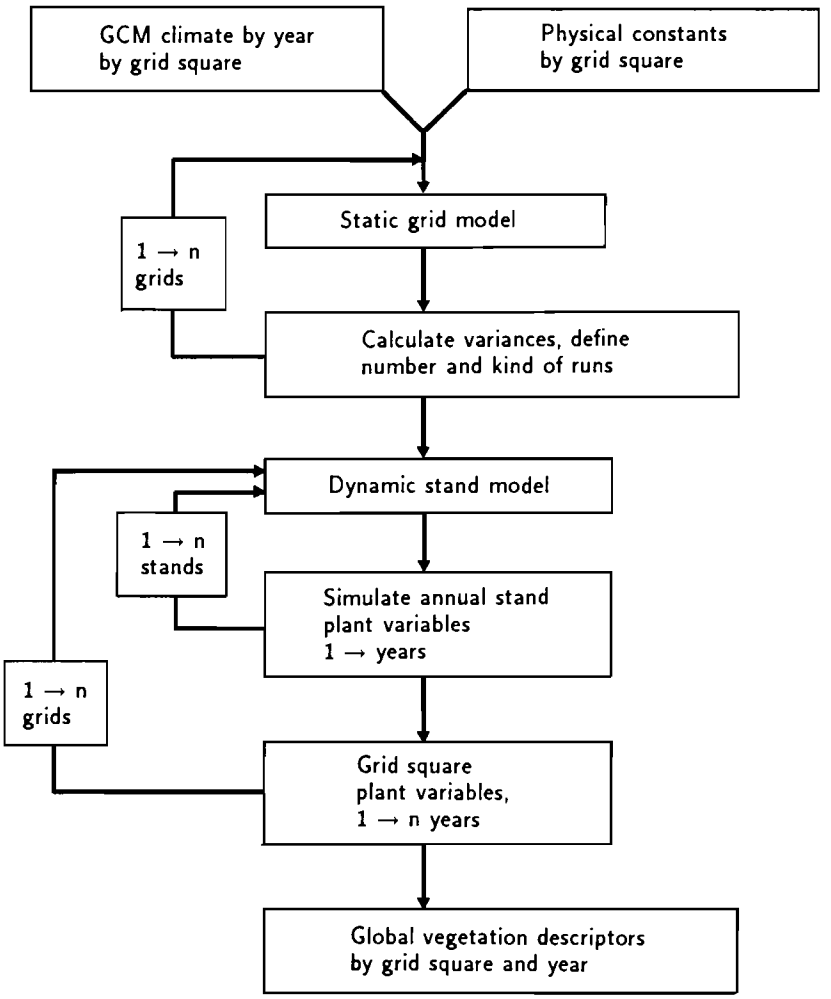

Figure 1. Flow diagram of a global vegetation change model. Static grid model component provides the geographically realistic spatial dynamics, while the dynamic stand model component characterizes the timing of spatial change within the global vegetation model.

number of patches as a stochastic process, and presents possible ways of incorporating interactions between patches through dispersal and mass effects.

With these components, the dynamics of natural and semi-natural vegetation can be modeled stochastically at landscape scale (*circa* 10^2–10^4 km^2) by simulating a large sample of patches, given estimates of the means, variances, and covariances of environmental variables and functions relating disturbance probabilities to these variables. This approach is diagramed in *Figure 1.* The first stages lead to the calculation of boundary conditions for a number of patch model runs, based on statistical distributions of climate, soils, topography, and

other physical features within each grid square. The patch model is then run under the defined conditions, to provide *samples* of vegetation dynamics in each grid square. This Monte Carlo approach provides a way to bridge the gap between the fine patch-scale of plant interactions that govern vegetation's successional responses to climatic change and the much broader scale resolved by atmospheric general circulation models. We believe this is a natural and theoretically sound approach, in that the processes controlling vegetation's internal dynamics (succession and stability) are to be found on the patch scale. Unlike the fluids studied in atmospheric and oceanic modeling, vegetation is immovable. Many processes of interest on the scales of watersheds, landscapes or biomes emerge from dynamics on the patch. In our model strategy, dynamics on the scale of patches are accumulated to generate emergent properties on the scale of a region or the globe.

Global vegetation models should be capable of projecting not only the effects of climate on vegetation but also the effects of anthropogenic changes in climate, vegetation, and soils on water resources. But adequate parameterization of surface hydrology requires a more mechanistic approach to water partitioning than has been attempted in existing vegetation models and more consideration of soil variation than has been attempted in atmospheric models. Section 4 deals with parameterizations of surface hydrology for use in the modeling approach outlined above. We also present a sketch of how a soil classification can be used to provide data for soil moisture accounting on the spatial scale required by global vegetation models.

Using an appropriate geographic information system, the effects of climatic change on potential vegetation type, net annual growth, and crop growth potential can be projected for hypothetical equilibrium conditions. These kinds of analyses are briefly reviewed in Section 5. This static approach can be implemented relatively quickly. It is the most important part of the modeling effort from the standpoint of those areas where artificial or intensively managed vegetation dominates and natural vegetation dynamics do not apply.

Section 6 describes environmental data needed in global vegetation analysis and systems to manage and analyze them. Similar capabilities are required to organize and interpret model results. We conclude in Section 7 with remarks about broad issues not covered in specialized sections.

2. Boreal Forest Models

2.1. Background

The ecological consequences of climatic change can be enormous (Emanuel *et al.*, 1985; Solomon, 1986), yet little work has been done to explore regional effects on specific forest biomes. Forest succession or gap models are suitable tools for this purpose (Botkin *et al.*, 1972; Shugart, 1984). These stochastic models simulate changes in forest composition and structure on patches of about 400–1000 m^2 by simulating mixed-species tree populations and their interactions with the environment through changes in the availability of light, water, and nutrients.

Gap models can simulate natural succession after disturbance, gap-phase replacement, and transient responses to climatic change. They are effective in describing the dynamic properties of forests from subarctic Alaska to subtropical Queensland and semiarid Southern Africa (Shugart, 1984). Conceptually similar models have been applied to non-forest vegetation, for example dwarf shrub heath (Prentice *et al.*, 1987). Although models developed for different regions and vegetation types have many common features, the details of processes and parameter requirements vary somewhat, restricting broad regional application.

Bonan and Shugart (1989) documented the features of boreal forest dynamics and its environmental controls, and Bonan (1988a and 1988b) constructed a forest stand simulation model to test this concept. The model's environmental modules reproduce seasonal patterns of solar radiation, potential evapotranspiration, and soil freezing and thawing for different topographic situations around Fairbanks, Alaska. They also simulate regional patterns of annual solar radiation, annual potential evapotranspiration, and the presence or absence of permafrost at locations in the boreal forests of North America, Scandinavia, and the Soviet Union. The model correctly simulates forest structure and vegetation patterns for several conifer, hardwood, and mixed conifer-hardwood forests in climatically different locations along a transect from Alaska to Newfoundland.

Figure 2 indicates the present and planned structure of the boreal forest model. The following paragraphs describe aspects of this model and work to increase its range of applicability with the goal of simulating regional responses to climatic change throughout the circumpolar boreal forest.

2.2. Description of forest growth

Gap models simulate forest stands as a series of independent patches. Each patch has its own tree population composed of different species, ages, and sizes. All individual trees on a patch interact with each other by competing for available resources. Individual trees are characterized by species, diameter, height, leaf area, and age. Thus vegetation structure (size distributions and tree canopy profiles) is described, and secondary variables – such as basal area, density, and biomass – can be calculated from the state variables.

In most gap models, including that used by Bonan (1988a and 1988b), individual tree growth is affected by light competition only insofar as the tree is shaded by taller trees (Shugart, 1984). The leaf area of each simulated tree is thus concentrated at the top of the stem – it is shaded by all taller trees and shades all shorter trees. While this pole and disk tree model is a reasonable initial representation of many temperate deciduous tree crowns, it is not appropriate for boreal forest conifers with crowns that extend down the stem. Leemans and Prentice (1987) developed a boreal forest gap model, FORSKA, that uses vertically distributed tree crowns (a cylinder tree model).

This more explicit simulation of vertical structure may be an important refinement for boreal forests because the narrow, vertically extended crowns of boreal trees and low sun angles at high latitudes mean that incoming radiation is effectively shared among many trees. One consequence is that single tree gaps

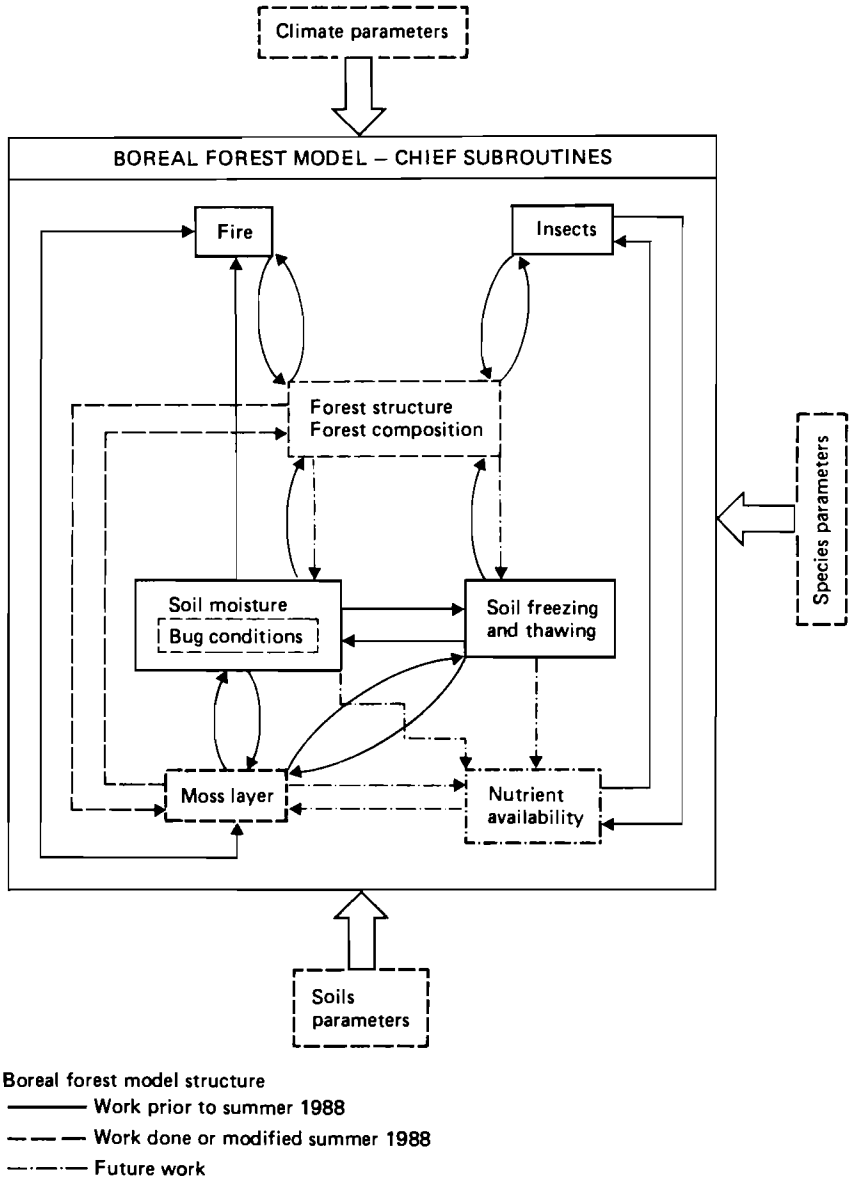

Figure 2. Present and planned boreal forest model structure. Work prior to 1988 is described by Bonan (1988a and 1988b). Work during summer 1988 is described in this report.

rarely bring enough light to the forest floor to allow a gap-phase regeneration cycle as seen in many lower latitude forests. Instead, it takes the synchronous death of several trees to allow regeneration of shade-intolerant species and a new sere to begin.

The FORSKA model provides a robust simulation of successional processes in forests of Central Sweden. Its robustness and modest demands for species-specific data make it appropriate as the core vegetation growth description in a general boreal forest model. We are therefore completing a model in which Bonan's environmental process algorithms drive updated versions (Leemans and Prentice, 1989) of the FORSKA forest dynamics algorithms. Procedures developed by Korzukhin and Ter-Mikhaelian (1982) and Gurtsev and Korzukhin (1989) are being incorporated into a special-purpose variant of the model to adjust solar radiation attenuation as a function of solar elevation.

2.3. Moss layer dynamics

Many dark coniferous boreal forests of North America, Scandinavia and the USSR are characterized by a thick (30–50 cm) moss-organic layer on the forest floor. This moss layer is an important structural component of boreal forests; it controls energy flow, nutrient cycling, water relations, and through these, stand productivity and dynamics (Bonan and Shugart, 1989). For example, soil temperatures and depth to permafrost are related to the thickness of the moss-organic layer. Its low bulk density and thermal conductivity insulate the mineral soil, lowering soil temperatures, maintaining a high permafrost table, impeding soil drainage, and promoting slow rates of tree growth and organic matter decomposition. With their high capacity to absorb water, mosses also absorb nutrients from precipitation efficiently, sequestering them from vascular plants until the mosses die and slowly decompose. During succession, the forest floor becomes the principal nutrient reservoir as nutrients are immobilized in the undecomposed organic matter. One of the consequences of warming may well be increased moss decomposition, which will produce drastic changes in the soil thermal and nutrient regimes of boreal forests.

The moss growth algorithm previously used by Bonan (1988a and 1988b) is not based on physiological characteristics. We developed a new algorithm based on a more detailed, physiological understanding of moss dynamics. The moss-organic layer is treated as two compartments, live (green) and dead (brown) moss, with dynamics given by the following equations:

$$\frac{dm_1}{dt} = q_1 m_1 [P_{max} p(\phi) - (R + b)] \tag{1}$$

$$\frac{dm_2}{dt} = q_1 b m_1 - a m_2 \quad , \tag{2}$$

where m_1 and m_2 are the biomasses of green and brown moss respectively; q_1 is a conversion factor from leaf biomass to leaf surface area; P_{max} is the maximum (unshaded) gross assimilation per unit leaf area; $p(\phi)$ describes the reduction of assimilation as a function of light intensity, ϕ; R is the respiration rate per unit leaf area; b is the decay rate per unit leaf area, and a is the annual decomposition rate. The light response function $p(\phi)$ is a hyperbola,

$$p(\phi) = a_1 \frac{\phi - a_3}{1 + a_2\phi} \quad , \tag{3}$$

where ϕ is the average amount of light in the moss layer:

$$\phi = \phi_0 e^{-k_i(q_1 m_1/2)} \quad . \tag{4}$$

ϕ_0 is light intensity at the top of the moss layer and k_i is a light extinction coefficient.

q_1 can be estimated by assuming that $dm_1/dt = 0$ when $m_1 = M_1$ (maximum green biomass):

$$q_1 = -\frac{2}{kM_1} \ln\left[\frac{a_3 + x}{1 - a_2 x}\right] \quad , \tag{5}$$

where

$$x = \frac{R + b}{P_{max} a_1} \quad .$$

b can be estimated by assuming that $dm_2/dt = 0$ when $m_2 = M_2$ (maximum brown biomass):

$$b = \left[\frac{a}{q_1}\right]\left[\frac{M_2}{M_1}\right] \quad . \tag{6}$$

Typical parameter values are listed in *Table 1.*

A thick (5–8 cm) moss layer precludes successful regeneration of many species of *Pinus*, *Betula*, *Picea*, and *Populus.* Other species (e.g., *Pinus sibirica*) require a thick layer for successful regeneration. Trees also have strong effects on moss productivity. Mosses thrive in moist, shaded conditions. Consequently, as a forest canopy becomes more open, moss productivity declines. If however, the canopy is too dense, mosses will be shaded out. Dense deciduous leaf litter also prevents the establishment and growth of mosses.

We have begun to analyze the consequences of these moss-tree interactions for forest dynamics. We combined Bonan's original forest growth model with the new moss growth algorithm described above [see *Figure 3*(*a*)], to simulate forest dynamics along soil temperature and soil moisture gradients in the forests around Fairbanks, Alaska.

Preliminary results suggest a wide range in moss-forest dynamics depending on site conditions [see *Figure 3*(*b*)]. On extremely cold, wet sites a thick moss layer develops, precluding tree growth. On slightly warmer sites, a thick

Table 1. Moss-layer model parameters.

Parameter	*Value*	*Units*	*Source*
a_1	3.41		Larcher, 1983
a_2	2.14		Larcher, 1983
a_3	0.08		Larcher, 1983
P_{max}	0.48	$kg \cdot m^{-2} \cdot yr^{-1}$	Larcher, 1983
R	0.12	$kg \cdot m^{-2} \cdot yr^{-1}$	Larcher, 1983
a	0.02	yr^{-1}	Van Cleve *et al.*, 1983
M_2/M_1	2		
$M_1 + M_2$	10	$kg \cdot m^{-2}$	Van Cleve *et al.*, 1983
b	0.04	$kg \cdot m^{-2} \cdot yr^{-1}$	
q_1	1.0	$m^2 \cdot kg^{-1}$	
k	0.90		

(20–30 cm) moss layer still dominates the vegetation, but *Picea* can grow. On warm, mesic sites the forest is initially dominated by *Betula* and *Populus*. Trees of these species prevent the formation of a moss layer. As they die and are replaced by longer-lived, shade-tolerant *Picea* trees, a thin (5–10 cm) moss layer grows on the forest floor. On warm, dry sites the forest is completely dominated by *Betula* and *Populus* and mosses cannot grow.

Graphs showing the sequence of annual moss biomass versus annual spruce biomass increments (phase plane analysis) suggests that in the absence of forest fires there is one equilibrium point of moss-*Picea* biomass on the cool, wet site [*Figure 3*(*c*), right]. With no initial moss or *Picea* biomass, the trajectory results in a *Picea*-dominated forest with a thin moss layer. When the initial *Picea* biomass is large enough, the dense canopy does not allow enough light to the forest floor for moss growth. But this forest structure is unstable, and as the initial spruce canopy breaks up, available light increases and allows moss growth [*Figure 3*(*c*), right]. When the initial moss biomass is too large, *Picea* regeneration is inhibited. But the lack of a forest canopy allows too much light onto the moss layer, creating dry conditions. Moss growth is reduced, and the moss layer slowly decomposes. When the depth of this layer decreases to a critical level, *Picea* regeneration begins [*Figure 3*(*c*), right].

Similar dynamics occur on colder, wet sites [*Figure 3*(*c*), left]. The major difference is that the forest composition has changed from a closed-canopy *Picea* forest to an open-canopy *Picea* woodland dominated by moss. In addition the net growth of mosses might be high enough under cold, wet conditions that a large, initial moss biomass would be a stable equilibrium point. This work has been documented in a manuscript submitted for publication in late 1988 (Bonan and Korzukhin, 1989).

2.4. Bog dynamics

Bogs and bog-forests are common through much of the lowland boreal zones of North America and the USSR. Bonan's boreal forest model treats upland forest dynamics and cannot simulate bog and bog-forest vegetation; however, a detailed

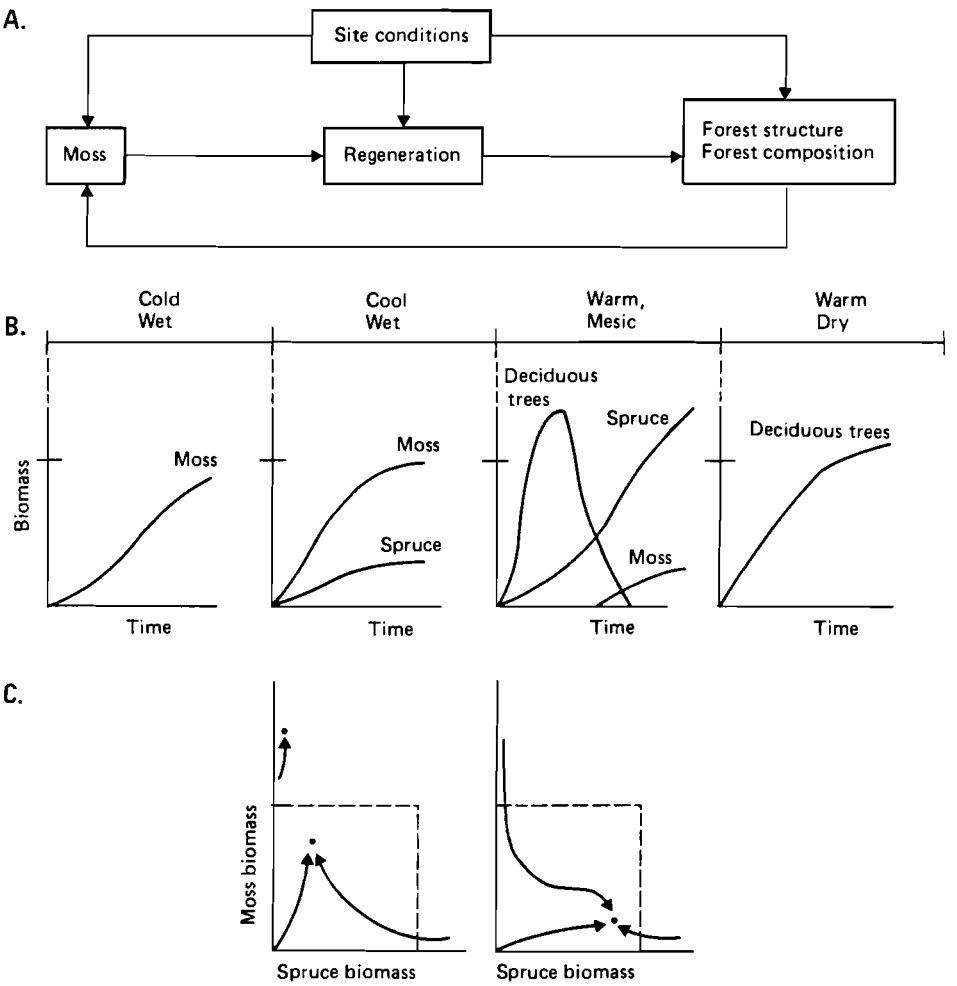

A: Moss–forest interactions
B: Moss–forest dynamics along environmental gradient
C: Phase plane trajectories for cool, wet site and warm, mesic site

Figure 9. Modeled moss-tree interactions in forest dynamics.

model of boreal zone bog-forest dynamics has been developed by Antonovsky *et al.* (1987a). We used aspects of the model to develop a simple algorithm to describe bog dynamics that is compatible with the spatial and temporal scales and parameter requirements of gap models.

Bog models must treat a layer of live moss and a layer of dead moss. The overall dynamics of the live moss layer is controlled as described above. The dynamics of the dead moss layer is controlled by the height of the dead moss layer, h_2, in relation to the height of the water table, h. When $h_2 < h$, anaerobic conditions preclude decomposition of dead moss. When $h_2 > h$, the part of the

dead moss layer that is above the water table (the active peat-forming layer) decomposes, while the part below does not – or does so at a much slower rate.

In a gap model, optimal tree growth and regeneration should be reduced as the water table rises and anaerobic soil conditions increase. Species differ in their response to anaerobic soil conditions; a first approximation to this difference in the model is handled by classifying species according to their ability to grow on bogs.

2.5. Model comparisons

Antonovsky and Korzukhin (1986) and Korzukhin *et al.* (1987 and 1989a) describe dynamic forest growth models for some boreal forests in western Siberia. These are age-class models that simulate behavior of trees in a given cohort, rather than individual trees. As with gap models, these models simulate the dynamics of an average forest plot sampled from a large spatial area. They do so by simulating the dynamics of the average plot, rather than simulating a range of forest trajectories and averaging.

We have initiated a comparison of gap models with these age-class models to examine the ecological consequences of the different formulations. The test forests are *Pinus sibirica* forests in west Siberia. These forests are described in detail by Kataeva and Korzukhin (1987), and primary stand data are available for comparison with model output.

2.6. Silvicultural and climatic requirements of boreal forest trees

The largest areas of continuous boreal forests in the world are in Fennoscandia and in the USSR, but there are little published data in English on most of the main trees of this region. There has been no previous attempt to synthesize silvicultural data on these taxa for use in forest succession models. We brought together data on 27 such species from Finnish, Russian, German, and Swedish literature, and compiled them in a form suitable for use in boreal forest models (Helmisaari and Nikolov, 1989). A preliminary report describing the detailed silvics of a few Siberian tree species (Korzukhin *et al.*, 1989b) was also produced. The work described here forms the first step toward publication of a circumboreal database of silvical and climatic information on boreal and boreonemoral trees.

A list of species was prepared from distribution maps (Anonymous, 1984) and other literature. Eleven tree species are landscape dominants: *Abies sibirica* Ledeb., *Betula pubescens* Ehrh., *Betula verrucosa* Ehrh., *Larix dahurica* Turcz., *Larix sibirica* Ledeb., *Larix sukaczewii* Dylis., *Picea abies* (L.) Karst., *Picea obovata* Ledeb., *Pinus sibirica* Rupr., *Pinus silvestris* L., and *Populus tremula* L.

We also considered 16 additional species that occur along the southern border of the boreal zone, or have a more restricted distribution within it: *Abies sahalinensis* Mast., *Alnus glutinosa* Gaertn., *Alnus incana* Willd., *Carpinus betulus* L., *Fagus silvatica* L., *Larix decidua* Mill., *Larix kurilensis* Mayr., *Picea*

Table 2. Boreal model species-specific parameters.

Symbol	*Explanation*	*Units*
ETS_{max}	Maximum annual effective temperature sum	°C days
ETS_{min}	Minimum annual effective temperature sum	°C days
T_{cold}	Mean temperature of the coldest month at continental boundary of geographic range	°C
Age_{max}	Maximum recorded age	Years
D_{max}	Maximum recorded diameter at breast height	cm
H_{max}	Maximum recorded height	m
H_{inc}	Maximum annual height increment	m
D_{inc}	Maximum annual diameter increment	cm
Moist	Soil moisture preference	1 : dry 2 : moist 3 : wet
Tol_{light}	Shade tolerance class	0 : intolerant 0.5 : intermediate 1 : tolerant
Tol_{nutr}	Nutrient stress tolerance class	0 : intolerant 0.5 : intermediate 1 : tolerant
Tol_{fire}	Fire tolerance class	0 : intolerant 0.5 : intermediate 1 : tolerant
Tol_{flood}	Flooding tolerance class	0 : intolerant 1 : occasional flooding 2 : seasonal flooding 3 : year-round flooding
Bog	Growth on bogs	0 : none 1 : bad 2 : good
Frost	Growth on permafrost	0 : bad 1 : good
Seed	Seeding year frequency	%
Soil	Mineral soil regeneration requirement	True or false
Moss	Moss layer regeneration requirement	True or false
Disp	Seeds dispersed by wind	True or false
Fire	Fire regeneration requirement	True or false
Drought	Seedling drought tolerance	True or false
Light	Minimum light intensity for seedling growth	%
Layer	Vegetative reproduction by layering	True or false
Stump	Tendency for stump or root sprouting	Mean sprouts per tree
$Sprout_{min}$	Minimum diameter sprouting	cm
$Sprout_{max}$	Maximum diameter sprouting	cm
$Slope_{HD}$	Initial slope of the height-diameter curve	$m\ cm^{-1}$
LSAR	Leaf area – sapwood area ratio	$m^2\ cm^{-2}$
Litter	Litter quality class	0 : bad 0.5 : intermediate 1 : good

ajanensis Fisch., *Picea koraiensis* Nakai., *Picea orientalis* (L.) Link., *Picea schrenkiana* Fish and May, *Pinus koraiensis* Sieb. and Zucc., *Pinus pumila* Reg., *Quercus mongolica*, *Quercus robur* L., and *Tilia cordata* Mill.

For each of these 27 species, we collected data on systematic classification (including races and hybrids), spatial distribution, habitat requirements (climate, soils, and associates), life history (reproduction and growth patterns, including maximum values for height, diameter at breast height, and age), response to environmental factors (soil moisture, nutrients, light, frost, permafrost, fire, wind, and flood), and enemies and diseases. The geographic distributions of the species were also compared with maps of annual effective temperature sum (5° C base) and mean temperature of the coldest month to derive climatic limits. This information was then used to assign values of 28 parameters for each species; these are listed in *Table 2*.

3. General Vegetation Models

The states of individual plants are not important on larger spatial scales. Models that describe population changes for each plant type are likely to be satisfactory for continental- to global-scale applications, providing the major features of vegetation structure and dynamics are simulated realistically. The computational requirements of population models can be substantially less than those of individual based models, allowing Monte Carlo solutions that sample the spatial variability in underlying model parameters.

3.1. A population based vegetation model

Key features of the individual-based forest stand models initially described by Botkin *et al.* (1972) and later by Shugart (1984) can be incorporated into analogous, population-based models. The state description of the community can be the number of individuals in layers above the simulated land unit. As in individual-based models, the land unit, referred to as a patch, is sufficiently small that light and other resources can be assumed to be horizontally homogeneous – patch sizes of about 400–1000 m^2 are appropriate for forests and smaller patch sizes for short vegetation.

In the model described here, the population in each layer is updated annually to reflect birth, growth, and mortality. The advancement of individuals through height layers is stochastic. The leaf area of each population is assumed to be uniformly distributed in height, and the probability of transfer into higher layers is derived from a mean height increment for the population of each plant type. The increment is species specific, and depends on current leaf area and size, and on environmental conditions. The emphasis on plant height and the assumption of homogeneity within height layers for each plant type or species are conducive to incorporating plant types other than trees, including types such as clonal grasses, for which a growth description based on individuals would be unworkable or irrelevant.

Model vegetation is composed of m types, designated $j = 1, 2, \ldots, m$. These may correspond to species, groups of species, or functional types. Conceptually, the total leaf area of each plant is concentrated at one height, and plant growth corresponds to an increase in that height. The space above the vegetation patch is divided into n arbitrary width layers designated $i = 1, 2, \ldots, n$. H is height above ground level, and H_i is the height of the upper boundary of layer i. The upper boundary is defined to be within the layer below it; so that if $H_{i-1} < H \leq H_i$, then H is within layer i. $H_0 = 0$, and corresponds to ground level.

The state of the community is described by the number of individuals of each type in each layer, p_i^j. Growth, recruitment, and mortality cause population changes that are evaluated at one-year steps. For each layer and plant type,

$$\Delta p_i^j = \sum_{k=1}^{i-1} I_{ki}^j - \sum_{k=i+1}^{n} I_{ik}^j + I_{0i}^j - I_{i0}^j$$
$$i = 1, 2, \ldots, n \tag{7}$$
$$j = 1, 2, \ldots, m \quad ,$$

where I_{ik}^j is a transfer of individuals of type j from layer i into layer k due to height increase. I_{0i}^j and I_{i0}^j are increases and losses in the number of type j individuals in layer i due to recruitment and mortality.

The transfers I_{ik}^j are derived from a height increment appropriate for a single individual with leaf area at the middle of the layer. This approach permits the use of the basic growth equations used in individual-based forest simulation models. For each plant type, the height increment depends on environmental conditions including available light, air temperature, soil moisture, and nutrient availability:

$$\Delta H_i^j = g_j(H_i', M)$$
$$j = 1, 2, \ldots, m \quad . \tag{8}$$

H_i' is the height of the middle of layer i:

$$H_i' = (H_i + H_{i-1})/2 \quad , \tag{9}$$

and M is a combined index of environmental effects. A height-increment function for woody plants is described later.

The height distribution of plants within layers is assumed to be uniform, and the transfers to higher layers I_{ik}^j are random variables. The probability that individuals of type j are transferred from layer i is derived from the increment ΔH_i^j given by equation (8):

$$P_i^j = \begin{cases} \Delta H_i^j/(H_i - H_{i-1}), & \text{if } H_{i-1} + \Delta H_i^j < H_i \\ 1, & \text{otherwise} \end{cases} . \tag{10}$$

The total number of individuals of type j transferred out of layer i is a binomially distributed random variable,

$$I_{iT}^j = B(P_i^j, p_i^j) \quad , \tag{11}$$

where $B(\cdot, \cdot)$ is the binomial distribution function.

Individuals of each plant type j transferred from layer i are placed in higher layers according to the degree of overlap if layer i were displaced by the height increment ΔH_i^j. Let u designate the layer containing the repositioned upper boundary of layer i, $(H_i + \Delta H_i^j)$, and l designate the layer containing the repositioned lower boundary, $(H_{i-1} + \Delta H_i^j)$. If $u \neq l$, then

$$I_{iu}^j = \frac{\left[(H_i + \Delta H_i^j) - H_{u-1}\right]}{(H_i - H_{i-1})} I_{iT}^j \tag{12}$$

$$I_{ik}^j = \frac{(H_k - H_{k-1})}{(H_i - H_{i-1})} I_{iT}^j \tag{13}$$

$$k = l + 1, l + 2, \ldots, u - 1$$

$$I_{il}^j = \frac{\left[H_l - (H_{i-1} + \Delta H_i^j)\right]}{(H_i - H_{i-1})} I_{iT}^j \quad . \tag{14}$$

If the height increment ΔH_i^j is sufficiently large so as to reposition part or all of layer i above the top of the top layer n, $H_i + \Delta H_i^j > H_n$, then the transfer into layer n is

$$I_{in}^j = \begin{cases} \dfrac{\left[(H_i + \Delta H_i^j) - H_{n-1}\right]}{(H_i - H_{i-1})} I_{iT}^j , & \text{if } H_{i-1} + \Delta H_i^j < H_{n-1} \\ I_{iT}^j , & \text{otherwise} \end{cases} . \tag{15}$$

If $H_{i-1} + \Delta H_i^j < H_{n-1}$, the transfers into layers below the top layer are given by equations (13) and (14). If the displaced layer i is within or coincident with one higher layer k, $u = l$, and all individuals are transferred into that layer:

$$I_{ik}^j = I_{iT}^j \quad . \tag{16}$$

3.2. Shading

Light intensity decreases downward through the plant canopy. The light intensity at each layer affects growth through the height-increment function, equation (8), and may affect other processes, such as recruitment. Light extinction is described by Beer's Law (e.g., Miller, 1981). Light intensity at height H is

$$\phi(H) = \phi_0 e^{-k\int_H^\infty l_i(h)dh} \quad , \tag{17}$$

where ϕ_0 is the intensity at the top of the canopy, and k is a constant light extinction coefficient. $l_i(h)$ is the leaf-area index (cumulative leaf area/patch size) at height H.

In the model framework pursued above, the leaf-area index in Beer's Law is expressed by

$$\int_H^\infty l_i(h)dh = \frac{1}{S}\left[\frac{1}{2}p_i^j l_a^j(H_i') + \sum_{k=i+1}^{n}\sum_{j=1}^{m} p_k^j l_a^j(H_k')\right] \quad , \tag{18}$$

where $l_a(H_k')$ is the leaf area of a plant of type j at the middle of height layer k. Leaf-area of an individual plant is related to height by a type specific function $l_a^j(H)$ – an example for woody plants is described below. S is the surface area of the patch. In keeping with the assumption that plant height is uniformly distributed within layers, one-half of the leaf area in layer i is included in the cumulative leaf area associated with that layer.

The effects of shading on growth are incorporated into the height-increment function through the growth multiplier M. As an approximation, the form of the response of annual growth to growing-season average light intensity is equated to the instantaneous response of net assimilation to light intensity represented by a rectangular hyperbola:

$$P(H) = P_{max}\frac{\phi_{abs}(H)}{\phi_{abs}(H) + \alpha} - R \quad , \tag{19}$$

where $P(H)$ is the net assimilation rate of leaves at canopy height H, P_{max} is the maximum (light-saturated) gross assimilation rate, $\phi_{abs}(H)$ is the light absorbed by leaves at canopy height H (less than $\phi(H)$ because leaves are oriented at various angles to light), R is the leaf respiration rate, and α is a parameter ranging from approximately 100 to 400 μmol·m^{-2}·s^{-1} – low values for shade tolerant plants, high for intolerants. The ratio P_{max}/α is the quantum efficiency of photosynthesis at low light intensity – about 0.05 (Jarvis and Leverenz, 1983). Leaf respiration R also tends to increase in proportion to P_{max}, so plants with small α also have low light compensation points:

$$R = \epsilon P_{max} \quad , \tag{20}$$

where ϵ is very roughly 0.1 (Larcher, 1983).

Differentiating Beer's Law, equation (17), yields the absorbed light intensity,

$$\phi_{abs}(H) = k\phi(H) \quad . \tag{21}$$

Equations (19)–(21) yield an expression for $P(H)$ that can be turned into a growth multiplier by dividing by the value of $P(H)$ corresponding to a typical growing-season average above-canopy light intensity in the region of optimal growth. This division eliminates P_{max}, leaving α as the single plant type-dependent parameter determining the response to light availability.

3.3. Recruitment and mortality

Recruitment and mortality, I_{0i}^{j} and I_{i0}^{j} respectively, can be complex functions of the vegetation state and environmental conditions. Both are usually random variables.

A simple recruitment function adds individuals only to layer 1 and depends only on available light at the middle of that layer:

$$\begin{aligned} I_{01}^{j} &= I_{01}^{j*} f_l^j \left[\phi(H_1')\right] \\ j &= 1, 2, \ldots, m \quad , \end{aligned} \tag{22}$$

where I_{01}^{j*} is the maximum recruitment for type j, a specified value. $f_l^j(\cdot)$ is a light response function.

Following the scheme for advancing individuals through height layers, the number of individuals removed from each layer due to mortality can be described by a binomially distributed random variable:

$$\begin{aligned} I_{i0}^{j} &= B(P_{i0}^{j}, p_i^j) \\ i &= 1, 2, \ldots, n \\ j &= 1, 2, \ldots, m \quad , \end{aligned} \tag{23}$$

where P_{i0}^{j} is the probability of mortality of individuals of type j in layer i.

3.4. Evaluation procedure

Equation (7) is evaluated on one-year time steps to simulate patch vegetation dynamics. Populations in each layer beginning with the top, $i = n, n-1, \ldots, 1$, are adjusted as follows:

- *Height increases.* Beginning with the top layer, $i = n, n-1, \ldots, 1$, populations are adjusted to reflect height increases. For each type, $j = 1, 2, \ldots, m$, height increment is evaluated for an individual at the middle of layer i, equation (8), and individuals are transferred to higher layers, $k = i+1, i+2, \ldots, n$, according to equations (12)–(16).
- *Mortality.* For each layer, $i = 1, 2, \ldots, n$, individuals of each type, $j = 1, 2, \ldots, m$, are removed due to mortality, for example, according to equation (23).
- *Recruitment.* Individuals of each type, $j = 1, 2, \ldots, m$, are recruited into each layer, $i = 1, 2, \ldots, n$, for example, according to equation (22). Recruitment may be restricted to particular layers.
- *Leaf-area profile.* The leaf-area profile, l_a^i, is adjusted to reflect the above population changes.

3.5. Growth formulations for woody plants

The derivation of a height-increment function, equation (8), applicable to trees, shrubs, and dwarf shrubs follows. If the allometric relation between leaf area l_a, crown diameter d_c, and height H is simplified to

$$l_a = k_1 d_c^2 \quad , \tag{24}$$

where

$$d_c = k_2 H \quad , \tag{25}$$

then

$$l_a = k_1 k_2^2 H^2 \quad . \tag{26}$$

Assume an asymptotic relation between height and stem diameter at ground level D

$$H = H_{max}\left[1 - e^{-k_3 D/H_{max}}\right] \quad . \tag{27}$$

The constants k_1, k_2, k_3, and H_{max} depend on the plant type. Presumably, k_1 is related to shade tolerance and k_2 to stature. Since H is proportional to D and l_a to D^2 during early growth, the constant relating l_a and H^2 can be obtained as C/k_3^2 where C is the initial value of the ratio l_a/D^2. Both C and k_3 depend on plant type. For example, k_3 is about 100 for many temperate trees but much larger for tropical forest pioneers. C can be obtained from the ratio of leaf area to sapwood area and is about 100–400, depending on wood anatomy and drought tolerance (Waring, 1983).

As in the growth equations derived by Botkin *et al.* (1972), a fixed fraction of net annual production is assigned to stem tissue and above-ground woody biomass is assumed proportional to D^2H. Net annual production is the difference between net assimilation and respiration by sapwood. Sapwood biomass is assumed proportional to $l_a(H + \frac{1}{3}d_c)$ according to the pipe model, and therefore to l_aH – because of the linear relation between d_c and H. This logic leads to the growth equation

$$\frac{d(D^2H)}{dt} = E_0 l_a (M - uh) \quad , \tag{28}$$

where $h = H/H_{max}$. E_0 is the growth efficiency of the plant type under optimum conditions and u is the proportion of optimal growth lost through respiration in non-photosynthesizing tissue when H approaches H_{max} and no other factors limit growth. The expression $(M - uh)$ is a *relative* growth efficiency (Leemans and Prentice, 1989). The value of this expression is an index of vitality (Waring, 1983) that can be used to adjust mortality rate. When this index falls below a critical (small) value, the probability of death is increased.

Combining the growth equation, equation (28), and relations among the sizes of different plant parts, equations (26) and (27), the rate of change of height is

$$\frac{dH}{dt} = \frac{3g(M - uh)h^2(1 - h)\ln^2(1 - h)}{(1 - h) + 2h\ln(1 - h)} \quad , \tag{29}$$

which has just three plant type-dependent parameters: g, u, and H_{max}. g is the initial (maximum) rate of height growth; it can be estimated easily for all types of woody plants.

3.6. Growth formulations for non-woody plants

At present we consider only two categories of non-woody plants, annual and perennial grasses. Because grasses are not dependent on the accumulation and maintenance of aboveground woody biomass to support and expand leaf area, they respond to environmental changes more rapidly than do woody plants.

Perennial grasses have two components of growth: a slow component (basal cover) and a fast component (height). Basal cover can change from year to year through tillering and establishment of new seedlings and therefore can follow environmental trends between years. But within any one growing season, the net production per unit basal cover depends on the height growth achieved that season. Thus we model the height growth in any one year as a function of the environment that year and use this to determine the change in basal cover from one year to the next; in this way we have a running estimate of annual production. As in the case of woody plants, environmental effects can be combined into a single multiplier affecting height growth.

Production of annuals is dependent only on the seed bank and the prevailing environmental conditions in any one growing season. If seed availability is not assumed to be limiting, then production of annual grasses can be modeled simply as a function of (a) the current year's environment, and (b) the availability of establishment sites, which in turn is inversely related to the basal cover of perennials. The conceptual formulation of the model including plant types of different stature is represented in *Figure 4*.

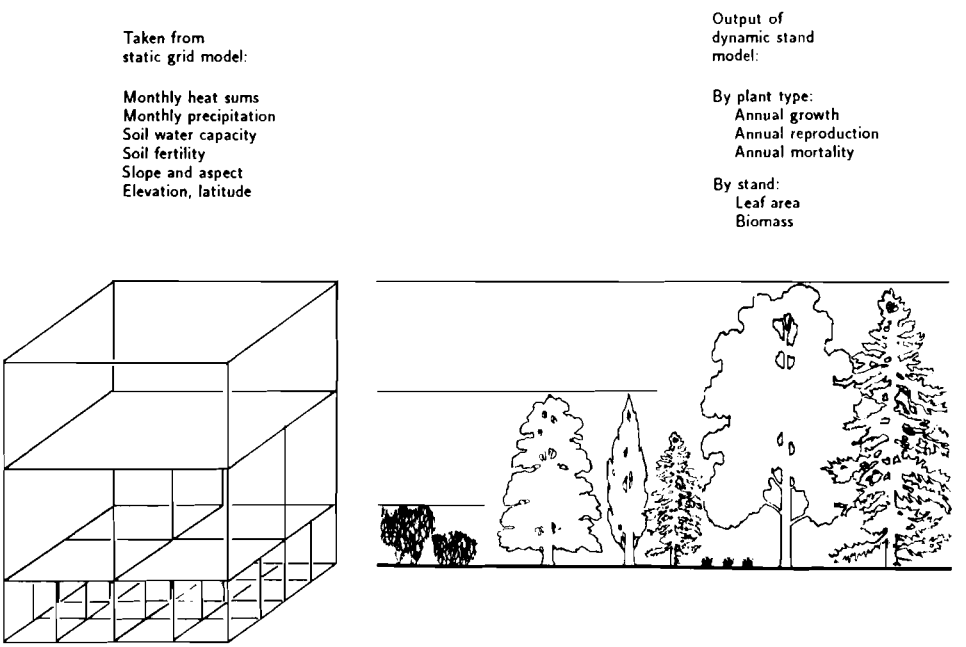

Figure 4. Conceptual form of the population model. The tallest plants shade out shorter ones; the number of simulations required for smaller-stature plants is greater than for tall plants. Each vertical layer of vegetation shown is subdivided into separate layers with growth in each layer calculated as in equation 7. The Static Grid Model referred to here is described in Section 5.

3.7. Functional classification of plants

Natural history characteristics (maximum height and age, shade tolerance, etc.) are not available for all species. Thus, the model of global vegetation dynamics must be formulated at a taxonomic resolution more coarse than species. We have attempted to implement plant functional types, introduced in models by Huston and Smith (1987). They defined a two-dimensional (light × water) environmental space. But rather than examining correlated patterns of plant distribution, they scrutinized patterns of growth response to the availability of these two resources.

This approach assumes the existence of two tradeoffs:

- Between maximum growth rate under high resource conditions (either water or light) and the ability to survive under conditions of low resource availability (Parsons, 1968; Grime, 1977; Chapin, 1980; Orians and Solbrig, 1977; Bazzaz, 1979; Huston and Smith, 1987; Tilman, 1988).
- The limit to the combined tolerance a plant can show for low availability of both resources.

These two sets of constraints were used to generate a surface representing the hypothesized relationship between maximum growth rate and the response to water and light availability (*Figure 5*).

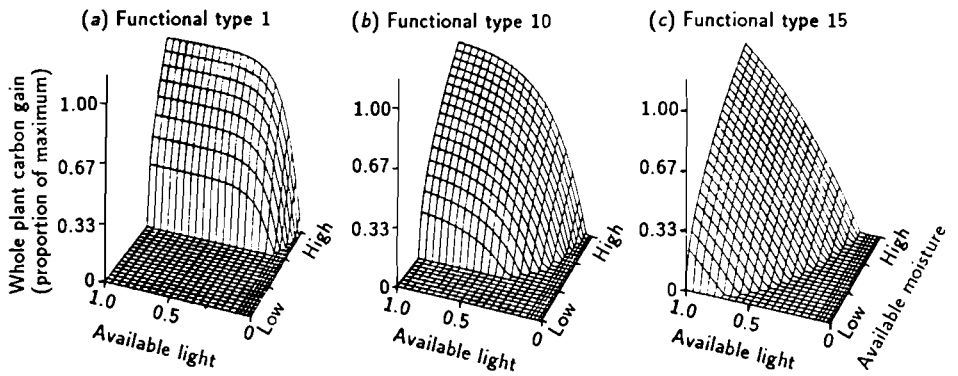

Figure 5. Relationship between maximum growth rate and response to water and light availability.

This surface was dissected into 15 evenly distributed functional plant types, whose dynamic interactions were examined in patch model simulations at various points along a hypothetical moisture gradient. This approach was able to account for general patterns of succession and physiognomy through a range of woody communities representing semi-arid woodlands to tropical rainforest (*Figure 6*).

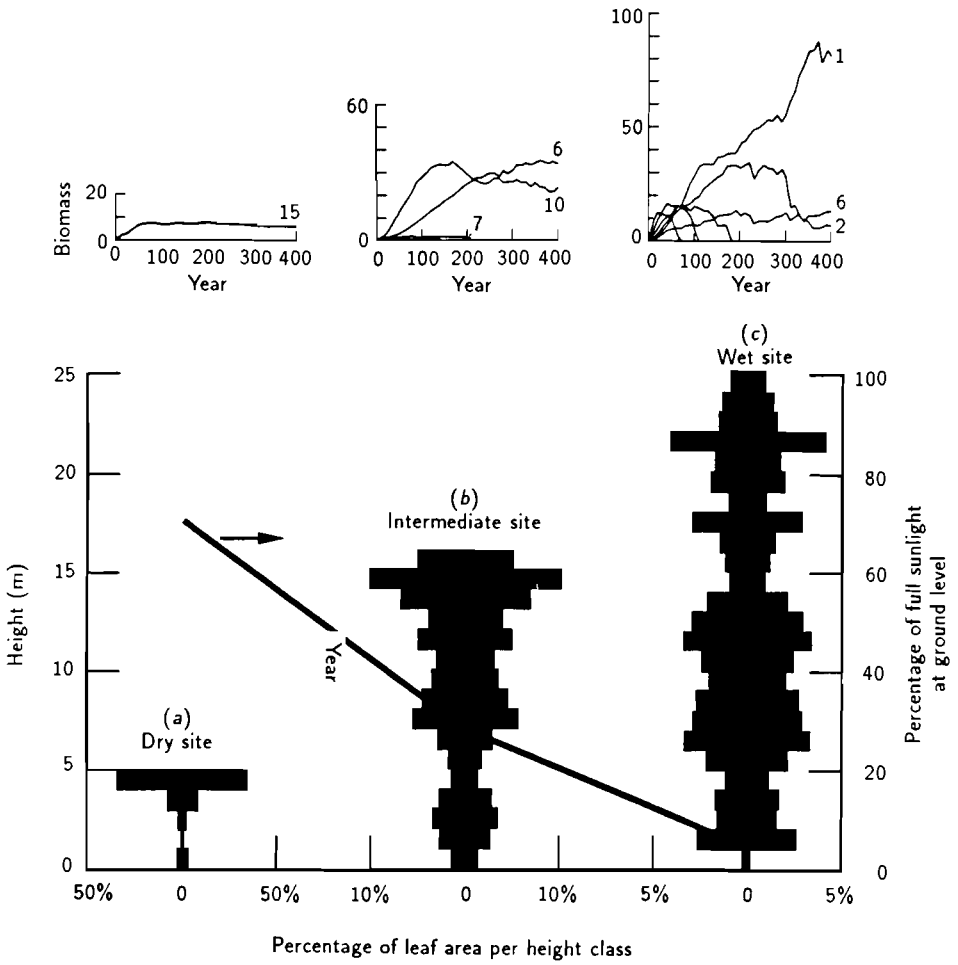

Figure 6. General successional patterns simulated by a patch model with 15 functional plant types: (*a*) as in competition among plant functional types along a moisture gradient; (*b*) as community leaf area on the same moisture gradient.

The approach of Huston and Smith can be extended to include mineral nutrients. Chapin (1980), Chapin *et al.* (1986), and Tilman (1988) discuss the patterns of tradeoff between growth rate and tolerance for species that have adapted to differing levels of nutrient supply. The constraints parallel those discussed for water, primarily because of the need to allocate carbon preferentially to root development at the expense of leaf area when nutrient availability is low. We can therefore add another constraint to the surface presented in *Figure 6*, with the highest growth rates being for plants with a low tolerance to reduced

levels of light, water, and nutrients. With increasing tolerance of any of these resources, there is an associated reduction in maximum growth rate, and there is a limit to the combined tolerance a plant can show for both light and nutrients (Tilman, 1988).

Together with water availability, air temperature forms the basis for most systems of global plant classification and for many concerns about changing global climate. Patterns of plant response to temperature are fundamentally different from those discussed for light, water, and nutrients. With the exception of species adapted to the most extreme environments, there is a correspondence in the levels of resource under which plants grow best (Ellenberg, 1954; Walter, 1973; Smith and Austin, 1989). Because of the positive feedback among supply, growth, and demand, most plants show an increase in growth with increasing availability of resources. This is not so for temperature. Temperature optima occur at very different points along the temperature gradient (e.g., Woodward, 1987). Plants can be classified according to their temperature requirements for optimal growth, independent of their responses to light, water, and nutrients.

Plants also differ in their tolerance of low winter temperatures, and these differences are related to the occurrence of different physiological mechanisms of cold tolerance (Woodward, 1987). Woodward shows that global physiognomic vegetation patterns can be predicted from climatic data using just three sets of limits: moisture requirements for sustaining a given leaf-area index, growing-degree day requirements for growth, and cold tolerances of different types of plants.

3.8. Modeling disturbance regimes

Natural disturbances that involve the destruction of plant biomass include fire, windstorms, avalanches, and floods (White, 1979). These may be catastrophic for individual patches of vegetation yet a normal part of the functioning of vegetation over broader areas. Vegetated landscapes are said to have a disturbance regime (Runkle, 1981) that can be modeled as a stochastic process with the disturbance affecting only some patches in any one time interval. One of the tasks in developing global vegetation models is to quantify probabilities of each major type of disturbance as a combined function of climate and vegetation state.

Here we focus on fire in the boreal forest. Boreal forest landscapes commonly consist of a mosaic of patches, each of postfire origin but of different successional ages. The structure and composition of this mosaic (its diversity, mean patch size, and age structure) depend on the fire regime. Fire probabilities depend not only on weather conditions, but also on vegetation conditions related to successional stage or age.

According to Heinselman (1973), the mean size of a single fire in the southern boreal forest of Minnesota is on the order of $10\,km^2$ and the maximum recorded size is about $500\,km^2$. Thus, landscape areas as large as $50\,km \times 50\,km$ can be considered independent of one another from the point of view of fire. This is not true however of smaller areas. Within such landscape areas, patches interact spatially through the propagation of fires. So there is an autocatalytic

effect within landscape areas by which the probability of ignition on any one patch increases with the probability of combustion on others.

The available data are insufficient to determine the form of the dependence of fire probabilities on forest structure or age (Ter-Mikhaelian and Furyaev, 1988). A more promising approach is through inverse estimation using a fire model (Antonovsky and Ter-Mikhaelian, 1987b). The way in which the model's parameters depend on climate can be estimated with the help of existing fire danger indices (Haines *et al.*, 1983). The approach of Antonovsky and Ter-Mikhaelian takes only severe fires into account. Some gap models allow fires of different intensities (Shugart and Noble, 1981; Kercher and Axelrod, 1984). A more mechanistic model would however take into account the effect of vegetation state on fire probabilities, which these models do not.

3.9. Dispersal and mass effects

Regeneration consists of three phases: seed production, seed transport and deposition, and seed establishment. Through seed production and dispersal, the probability of establishment of a species is influenced by the abundance of that species in the surroundings, either positively (a species that is abundant in a region may be able to maintain itself in marginal habitats by continual replenishment from more favorable habitats), or negatively (a species may be rare or absent, even in a favorable habitat, if located far from seed sources). The latter effect may be especially important when climate changes rapidly, allowing favorable habitats to extend a long way beyond species' previous range. In the context of global vegetation models, these *mass effects* come in as autocatalytic effects within landscape areas and as interactions between adjacent landscape areas.

Little is known about the mechanisms by which seeds disperse long distances and become established in new surroundings during rapid climatic change or in the colonization of new habitats. There are no quantitative data. On a large enough scale, dispersal can be represented as a quasi-exponentially decreasing function of distance. Grass species, for example, disperse roughly 90% of their seeds within a radius of a few meters around the parent plant, but beyond this the number of seeds dispersed is no longer well correlated with distance. Dispersal between patches can thus be modeled by making the probability of germination a function of climate and site characteristics (Horovitz and Schemske, 1986), and the probability of available seeds as a function of average abundance in the landscape. With some assumptions, this second function could be derived from the function relating dispersal probability to distance (Rabinowitz and Rapp, 1981). But dispersal between landscape areas is more difficult to model because of the problem of specifying long-distance dispersal probabilities; possibly some seeds should be allowed to disperse randomly into adjacent landscapes.

One part of a solution is to develop a mathematical model for the dispersal of plants with wind-distributed seeds. [The formulation should be as simple as possible. For example, Solomon and Harrington (1979) represented particle

dispersion as a function of four variables (particle fall-speed, source strength, source height, and windspeed), to calculate annual downwind deposition of pollen grains from montane sources:

$$N(X) = N(O) \exp - \left[\frac{V_g}{uH} X\right] \tag{30}$$

where $N(X)$ is deposition at distance X downwind, $N(O)$ is deposition at the particle source, V_g is particle deposition velocity, u is mean windspeed, and H is tree height.] Seed transport depends on meteorological conditions, particularly winds. In events such as tornados, thunderstorms, etc., seed transport over great distances is possible but could hardly be predictable. The transport of seeds in the atmosphere from different species varies significantly because of variations in the seed's wings, size, weight, and form. The natural transport of seeds also depends on soil characteristics, local relief, shapes of forest areas, orography, and deposition surface properties.

In the absence of such detailed information, the following assumptions were made. First, only non-extreme atmospheric conditions were considered. Second, migration of species could be represented by migration of a single tree. Third, all processes of secondary transport of seeds by wind (after their deposition to ground) were neglected. Only time-integrated fields of seeds concentration are considered.

Many dispersion models are available. Models relevant to seed transport have been developed for heavy particle dispersion on a local scale (up to 10 km). For example, the analytical solution of a prognostic equation for transport of heavy particles on a local scale was suggested by Berliand (1985). However, the simplest and most extensively used model for local scale dispersion is the Gaussian model. The concentration distribution from a single release is

$$q(x,y,z,t) = \frac{Q}{(2\pi)^{3/2}\sigma_x\sigma_y\sigma_z} \exp\left[-\frac{(x-\bar{u}t)^2}{2\sigma_x^2} \cdot -\frac{y^2}{2\sigma_y^2}\right] \left\{\exp\left[-\frac{(z-h)^2}{2\sigma_z^2} + \exp\left[-\frac{(z+h)^2}{2\sigma_z^2}\right]\right\}\right. \tag{31}$$

where $q(x,y,z,t)$ is a concentration of emitted particles, x, y, z are rectilinear axes, t is travel time, Q is total amount of material released at time $t = 0$, σ_x, σ_y, σ_z, are the standard deviations of the Gaussian distributions in the x, y, and z directions, $\bar{u}$ is the mean wind speed, and h is the height of release.

The time integrated concentration is given by the Gaussian plume model as

$$q(x,y,z) = \frac{Q}{2\pi\bar{u}\sigma_y\sigma_z} \exp\left[-\frac{y^2}{2\sigma_y^2}\right] \left\{\exp\left[-\frac{(z-h)^2}{2\sigma_z^2}\right] + \exp\left[-\frac{(z+h)^2}{2\sigma_z^2}\right]\right\} \tag{32}$$

The mean wind direction is taken to be the x-axis and the origin of the coordinate system is assumed to be at the release point. From the expression for concentration (equation 32), the ground level concentration is obtained by setting $z = 0$. Then, ground level concentration is

$$q(x,y,0) = \frac{Q}{\pi\bar{u}\sigma_y\sigma_z} \exp\left[-\frac{y^2}{2\sigma_y^2} - \frac{h^2}{2\sigma_z^2}\right] \tag{33}$$

Equation (33) gives the ground level concentration in the absence of material deposition. The deposition rate due to dry deposition is calculated using the concept of deposition velocity (e.g., IAEA, 1986), the ratio of deposition rate to air concentration. The deposition rate D_d is given by

$$D_d(x,y) = V_g q(x,y,z_r)$$

where V_g is the deposition velocity of seeds and z_r a reference height.

Measurements of deposition velocity usually relate to concentration at a height of one meter. For simplicity, however, most calculations assume $z_r = 0$.

Depletion correction to account for dry deposition is made by correcting for loss of material from the plume. The classical approach, called the source depletion model, assumes that the loss reduces the effective source strength. This has the unrealistic implication that turbulence instantly redistributes the airborne material so that the vertical Gaussian profile is maintained. This model is easy to use and still preferred to the recently developed surface depletion model (Horst, 1977) in which the vertical Gaussian profile is not maintained and the deposition loss is accounted for by assuming a negative source at ground level. However, the difference between the two models does not exceed 10–20% (Horst, 1977) and the source depletion model is mostly adequate.

The source depletion model assumes that the source strength at a given downwind distance is a function of wind direction x. The depletion of the source due to the deposition from x to $x + dx$ is

$$dQ_x = -V_g dx \int_{-\infty}^{\infty} q(x,y,z_r)dy \tag{34}$$

Taking the reference height z_r as 0 and using the form of concentration given by equation (33) with Q replaced by Q_x gives

$$dQ_x = \left[\frac{V_g}{u}\sqrt{\frac{2}{\pi}}\right]Q_x \cdot \frac{e^{-h^2/2\sigma_z^2}}{\sigma_z}\,dx \tag{35}$$

We shall assume that the deposition is occurring with the same V_g throughout the plume. Then expression [equation (35)] may be integrated to give the frequently quoted relations

$$Q_x = Q\ e^{-\left[\frac{V_g}{u}\sqrt{\frac{2}{\pi}}\right]\int_0^x \frac{e^{-h^2/2\sigma_z^2}}{\sigma_z}\,d\xi} \tag{36}$$

Substitution of equation (36) into equation (33) gives the model which we used for seed dispersion.

$$q(x,y,0) = \frac{Qe^{-\sqrt{\frac{2}{\pi}}V_g/u\int_0^x \cdot\, e^{-H^2/2\sigma_z^2 d\xi}/\sigma_x}}{2\pi\bar{u}\sigma_y\sigma_z}\ x\ e^{-y^2/2\sigma_y^2}\ e^{-H^2/2\sigma_z^2} \tag{37}$$

For computing equation (37) one should specify the dispersion parameters of the model. Following Doury (1976) we used the simple assumption that

$$\sigma_x = \sigma_y = d_1(x/u)\sigma_z = d_2(x/u)^{1/2} \tag{38}$$

The dispersion parameters d_1, d_2 are specified from the results of tracer experiments. We shall use the estimates of dispersion parameters from Fedorov and Pitovranov (1988), which were determined from the data of the Savannah River Laboratory (SRL) tracer experiment (Rodriguez and Rosen, 1984). All data of SRL tracer experiments were collected during daytime when stable atmospheric conditions were observed. (Seed dispersion happens mainly during windy atmospheric conditions, corresponding to stable atmosphere.) Therefore, parameters d_1 and d_2 were taken to equal 0.26 m/sec and 7.4 m/sec respectively.

The height of release and the total amount of released seeds depend on individual species characteristics and could be rather simply assessed for given species. Much more difficult is to find data describing dry deposition velocity of seeds for individual species. We have assumed that the velocity is some millimeters per second. The computer run has been made with the following parameters of equation (38): $h = 10$ m, $Q = 10^6$ seeds, $V_g = 0.1$ cm/sec.

Because we would like to assess the speed of species migration, it is necessary to define a threshold value of seeds per hectare above which we can assume that the probability of establishment (i.e., seed germination and seedling

survival) is high. Unfortunately, the literature provides no information to define such thresholds. Therefore, we assumed that this amount is equal to 10% of seed density per hectare recommended for species planting (e.g., Fowells, 1965). In the computation we suppose 10^3 seeds per hectare as the critical value. The shifting of the critical value boundary for various wind speeds can be seen in *Figure 7.*

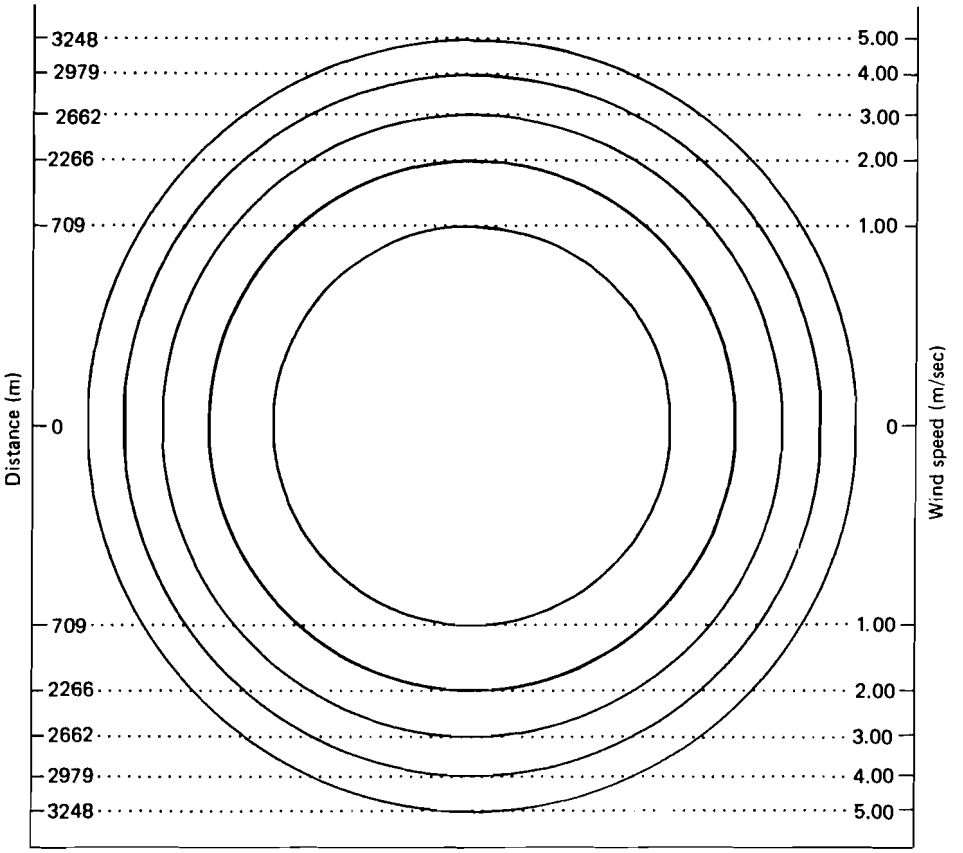

Figure 7. Change in the critical seed boundary for various wind speeds. The isopleths represent the distance from seed sources at which 10^3 seeds per hectare will occur at differing wind speeds.

The spatial distribution of species migration depends on the wind rose in any given area. An example of computation of species migration with a wind rose of three equal direction frequencies can be seen in *Figure 8.*

Incorporating dispersal into global vegetation models implies adding another dimension to the cross-classification of plants into functional types. We suggest the use of natural history compendia (e.g., Fowells, 1965) to develop correlations between dispersal strategies and successional roles.

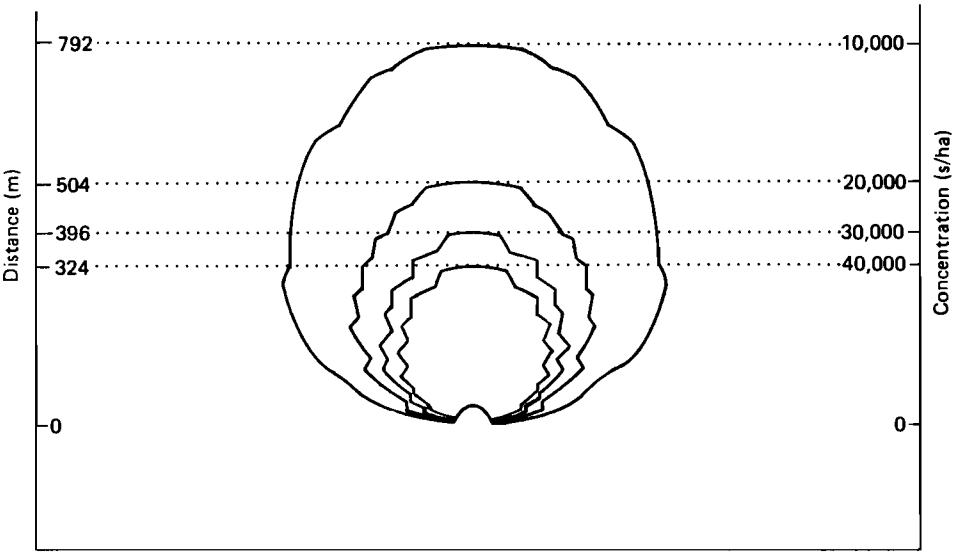

Figure 8. Seed distribution pattern as a function of seed characteristics and wind rose. Winds are equal from three directions (no wind from top of diagram). Isopleths represent deposition density of seeds, in seeds/hectare.

4. Surface Hydrology

The short branch of the hydrologic cycle that partitions precipitation into actual evapotranspiration (AET), storage, and runoff is an integral part of the global vegetation system. Plant growth and vegetation structure depend strongly on seasonal soil moisture patterns. The subannual dynamics responsible for these patterns must be treated in vegetation models even when applications focus on long time scales.

The hydrologic cycle description has three main components: (1) precipitation and potential evapotranspiration (PET) estimates from weekly or monthly climatic data, (2) a soil-moisture accounting scheme, and (3) a way of estimating reduction of the AET/PET ratio with decreasing soil moisture (Specht, 1972; Cramer and Prentice, 1988). The model should also be responsive to changes in vegetation properties that affect AET, including albedo, canopy conductance, surface roughness, and rooting depth. The feedback influence of plant cover on AET is fundamental to the interactions between plant types in regions where water is limiting, and to understanding the effects of vegetation changes in such regions on climate.

A variety of approaches relate AET and potential net primary production (NPP) (Box, 1981 and 1989; Lieth and Box, 1972). For example, there is an established relationship between annual NPP and AET:

$$\mathrm{NPP} = \Theta\mathrm{AET} \quad , \tag{39}$$

where Θ is an increasing function of foliar projective cover (FPC) that tends to an upper limit characteristic of a wide range of closed vegetation types (Hilmi, 1957; Rudakov, 1977). This function could be described empirically, and sustainable FPC calculated along lines suggested by Specht (1981). The problem of predicting FPC then reduces to estimation of annual AET. Kovacs' relation (Olejnik, 1988), provides one semi-empirical method. Another semi-empirical relation,

$$\mathrm{AET} = \mathrm{PET}\tan(P/\mathrm{PET}) \quad , \tag{40}$$

describes the dependence of annual AET on annual precipitation P and PET (Antonovsky *et al.*, 1988). A more mechanistic approach would be to find the equilibrium point (by simulation) of the AET model described below. Alternatively, Eagleson (1978) suggests an integrated methodology to estimate sustainable FPC and AET from data on climate and soils. The essential components of a daily AET model are described in the following paragraphs.

4.1. An AET model

Short-wave radiation at the earth's surface can be calculated from extraterrestrial insolation and times of sunrise and sunset by applying a semi-empirical description of the influence of atmospheric scattering and clouds (Prescott, 1940). Insolation, sunrise, and sunset are calculated from theoretical models (e.g., Swift, 1976). Long-term (millennial) changes can be treated by including the effects of orbital variations on the parameters of such models.

Surface radiation is partitioned into diffuse and direct components by an indirect method. The diffuse fraction is estimated from the ratio of short-wave surface radiation to insolation (Bristow and Campbell, 1982) and the direct-beam fraction obtained by subtraction. Slope factors from Swift's algorithm are applied to the direct-beam component, and the diffuse component is corrected for the fraction of visible sky. The total short-wave radiation incident on a slope at ground level is then the sum of direct and diffuse radiation and any reflected components from adjacent surfaces. An estimate of surface albedo is needed to estimate the reflected radiation, and to convert the total incident short-wave radiation to the total absorbed by the surface.

Net long-wave radiation is calculated, following Linacre (1968), as a semi-empirical function of mean temperature and cloudiness. We assume that net long-wave radiation on a slope is equivalent to net long-wave radiation on a horizontal surface. The net radiation for a slope is then simply the total absorbed short-wave flux minus the net (upward) long-wave flux.

Potential evapotranspiration is calculated from the Penman-Monteith equation but with daily values substituted for instantaneous values and with canopy resistance set to zero. The required data are net radiation, temperature, humidity, wind speed, and an estimate of surface roughness.

Actual evapotranspiration is calculated from PET and current soil moisture, using a simple form of the supply and demand approximation described by Federer (1982). Instantaneous AET is the lesser of evaporative demand, assumed equal to PET, and a supply rate, linearly related to the relative wetness of the rooting zone. Federer's simplest integration, which approximates the shape of the diurnal course of demand by a rectangle stretching between sunrise and sunset, can be used to obtain daily AET. This approach requires an estimate of the depth of the rooting zone – partitioning of water uptake among plant types with different rooting depths is not yet addressed.

In the simplest version of the model, each day's precipitation enters a reservoir corresponding to a standard soil with a specified water-holding capacity (we used 150 mm). When this bucket is full, all extra precipitation is lost as runoff. An alternative layered-soil model allows soil hydrologic properties to be characterized more accurately than in single reservoir models. In the layered model, maximum infiltration rates can limit the rate of downward penetration into the top layer, between layers, and from the bottom layer into deeper reservoirs. Precipitation that cannot enter the top layer is added to runoff. Water prevented from infiltrating into lower layers simply backs up the profile – runoff occurs when the entire profile is saturated.

4.2. Soil characteristics

Soils are differentiated into discrete layers with different hydrologic (and pedologic) properties – this is important when modeling the behavior of plants with different rooting depths. The maximum infiltration rate of any soil layer is a function of the void space per unit volume, which in turn is a function of the texture and structure of the material. The total amount of water that can be held in the layer depends on the void space per unit volume and the depth of the layer. Thus, total (effective) depth, the number of layers, the depth of each layer, and the maximum infiltration rate characteristic of each layer must be specified to characterize a soil. Some of this information can be derived from the FAO Soil Classification System (FAO/UNESCO, 1974); some must be derived from the general soils literature or from compilations of soil profile data.

Effective depth. Effective depth can be defined as the depth to which roots can penetrate and drainage is unimpeded. It is limited by the occurrence of bedrock or of indurated, impermeable layers (pans) or is given by the depth of the upper surface of the C horizon. Effective depth determines the depth of the rooting zone and the total water-holding capacity of the soil profile.

With the exception of Lithosols, soil types are not defined by depth to bedrock or effective depth. But some soil types are characteristically shallow (e.g., rendzinas and rankers tend to be less than 0.5m deep). Maximum effective depth needs to be estimated for the other soil types. Additional information on maximum effective depth can be obtained from some phase categories (e.g., those which indicate the presence of pans) and from slope classes (e.g., soils on slopes steeper than 30% tend to be shallow). The basic depth categories are:

- 0–0.1 m: Lithosols – soils that are limited in depth by continuous coherent hard rock within 0.1 m of the surface.
- 0.1–0.5 m: Rendzinas, Rankers, and lithic phases of all other soils – soils that have a continuous coherent and hard rock surface within 0.5 m of the surface. Soils on slope class c – steeply dissected to mountainous terrain with slopes over 30%.
- 0–1 m: Petrocalcic, petrogypsic, petroferric, and duripan phases – soils with a continuous cemented or indurated horizon within 1.0 m of the surface. These phases differ with respect to the cementing agent, calcium carbonate, gypsum, iron, and silica respectively.
- Fragipan phase – soils with a dense, seemingly cemented loamy horizon within 1.0 m of the surface. Although the fragipan is not strictly impermeable, it is only slowly or very slowly permeable and so limits drainage of the soil; the hardness of the layer also limits plant rooting depth.
- 0–1 m or deeper: All other soil types.

Effective depth can also be limited by groundwater. The influence of groundwater on the soil profile is indicated by hydromorphic properties including location of the groundwater capillary fringe at or near the soil surface for part or all of the year, the occurrence of a histic H horizon that reduces conditions within the soil profile, reduction and segregation of iron and hence the development of mottling, and neutral to blue soil colors. It is not clear how or whether to incorporate hydromorphically-determined limits to effective depth, since the groundwater table can vary in response to climatic change. The hydromorphically-determined effective depth categories are:

- 0–0.5 m all year: Gleysols – soils strongly influenced by groundwater with a reducing moisture regime virtually free of dissolved oxygen because of saturation by groundwater or its associated capillary fringe and with hydromorphic characteristics within 0.5 m of the surface.
- 0–0.5 m seasonally: Gleyic groups within the other soil types, including gleyic solonchaks, gleyic solonetz, gleyic greyzems, gleyic luvisols, gleyic podzoluvisols, gleyic podzols, gleyic phaeozems and gleyic acrisols – soils with lower horizons influenced by groundwater, or that have a seasonally perched water table within the profile, and hydromorphic characteristics within 0.5 m of the surface.
- 0–1 m seasonally: Gleyic cambisols – soils with an altered subsurface horizon that is not the result of mineral accumulation and that have hydromorphic properties within 1 m of the surface.
- 3–5 m all year: Phreatic phase – soils which have a groundwater table within 3–5 m of the surface such that the presence of groundwater is not reflected by the development of hydromorphic characteristics within the soil profile but does influence the water regime of the soil.
- >5.0 m all year: All other soils – soils in which the depth of effective drainage is not impeded by groundwater, perched water tables, or the capillary fringe associated with either of these.

Soil layers. Four functional soil layers are distinguished. The uppermost layer (O) is characterized by the accumulation of organic material and is equivalent to the H and O soil horizons. This layer is distinguished because organic accumulations at or near the surface of the soil have much higher water-holding capacity than the rest of the mineral soil. The second layer (A) is a mineral layer characterized by a mixture of humified organic matter and somewhat coarser texture than underlying material. The A layer is equivalent to the A and E soil horizons. The third layer (B) is an illuvial mineral layer and therefore characterized by finer or heavier textures than the overlying layers. This layer is equivalent to the B soil horizons. The lowest layer (C) is equivalent to the C soil horizon – the layer of unconsolidated, weathered material from which the soil is presumed to have developed. Layer C allows water to drain out of the profile.

The complete range of soil horizons may not occur in all soil types (e.g., rendzinas are characterized by poorly developed A horizons directly underlain by bedrock). In some cases therefore, there may be layers with zero depth.

Depth of the organic layer (O). The following classes are distinguished:

- >0.4 m: Histosols – soils characterized by an organic horizon of 40 cm or more either extending down from the surface or within the uppermost 0.8 m of the profile that is saturated with water for prolonged periods unless artificially drained.
- 0.2–0.4 m: Soils with a histic H horizon – soils with an organic horizon 20–40 cm thick either extending down from the surface or within the uppermost 80 cm of the profile that is saturated with water for prolonged periods unless artificially drained. Such horizons must occur in mollic, humic, and gelic gleysols.
- 0.0–0.4 m: Soils that may have a histic H horizon, fluvisols, solonchaks, mollic and humic planosols, and plinthic gleysols.
- 0.0–0.2 m: Soils with a discrete O horizon or an H horizon less than 0.2 m thick – such horizons can occur in (at least) chromic cambisols, humic podzols, orthic podzols, placic podzols, and humic acrisols.
- 0 m: All other soils – soils with no discrete organic accumulation layer.

Depth of the A and B layers. Rendzinas, lithosols, regosols, and histosols do not have distinct B horizons; the depth of layer A is therefore given by the effective depth minus the depth of layer O. All other soil groups have both A and B horizons, and therefore the depth of the A and B layers have to be specified. The depth of A (including E horizons where present) and B horizons are however not defined for individual soil types. The simplest way to define the depth of the A and B layers is to assume that they are of the same size, given by (effective depth – depth of layer O)/2.

Presence or absence of the C layer. This defines the nature of the bottom of the profile. If the effective depth is set by bedrock or an impermeable layer, then layer C is absent. Thus layer C is absent in Lithosols, Rendzinas, Rankers,

lithic, petrocalcic, petrogypsic, petroferric, duripan, and fragipan phases, and present in all other soils.

Maximum infiltration rates of each layer. These can be approximated from the characteristic bulk density and texture of each layer. They must be specified separately for the O and C layers. There is a basic division between those soils that have a marked textural contrast between the A and B horizons (i.e., soils that show an abrupt textural change between A and/or E horizons and the underlying B horizons), and soils with either uniform or gradational profiles (i.e., soils that show no textural change down the profile or that show only a gradual increase in texture). The maximum infiltration rates of the A and B layers must be specified separately for texture-contrast soils (acrisols, luvisols, solonetz, planosols, luvic yermosols, luvic xerosols, luvic kastanozems, luvic chernozems, luvic phaeozems, gleyic phaeozems, orthic luvisols, chromic luvisols, podzoluvisols, and nitosols) but could be assumed to be the same in uniform or gradational profiles.

5. Static Grid Analysis

The broad-scale distribution of major vegetation types or biomes is roughly in equilibrium with present climate. So at a coarse level vegetation can be related to climate by purely correlative methods. Similarly, the viability and potential yield of specific crops can be related empirically to climate, even though their actual distributions may be largely a human decision. In both cases – natural vegetation and crops – equilibrium models provide predictions of *potential* vegetation states. The pursuit of equilibrium vegetation (static grid) models complements the development of the dynamic models discussed thus far. Insights retrieved through either effort can reinforce the other.

The Holdridge Life-Zone system (Holdridge, 1947) is one empirical equilibrium model for natural vegetation. It classifies climate with names indicating the natural vegetation type usually associated with the climatic limits. Emanuel *et al.* (1985) computerized the Holdridge system and applied it to describe potential natural vegetation distributions under CO_2-induced warming. The Holdridge system is now being modified to use variables which may be more functionally important to vegetation than the variables used originally: temperature sums (growing degree days) in place of annual "Biotemperature," and simulated monthly soil moisture during the growing season (see Section 4), rather than annual rainfall (*Figure 9*). The data sets used for the static grid model (*Figure 9*) also provide input to the population models as diagramed in *Figures 1* and *4*, and are a necessary part of the global data analysis described in Section 6.

The potential geographic range of specific crops can be projected using the approach pioneered by the FAO Agro-Ecological Zone (AEZ) Project at IIASA, which aimed "to obtain a first approximation of the production potential of the world's land resources, and so provide the physical data base necessary for planning future agricultural development" (FAO, 1981). Soil and land-use constraints were assessed from the World Soil Map (FAO-UNESCO, 1974).

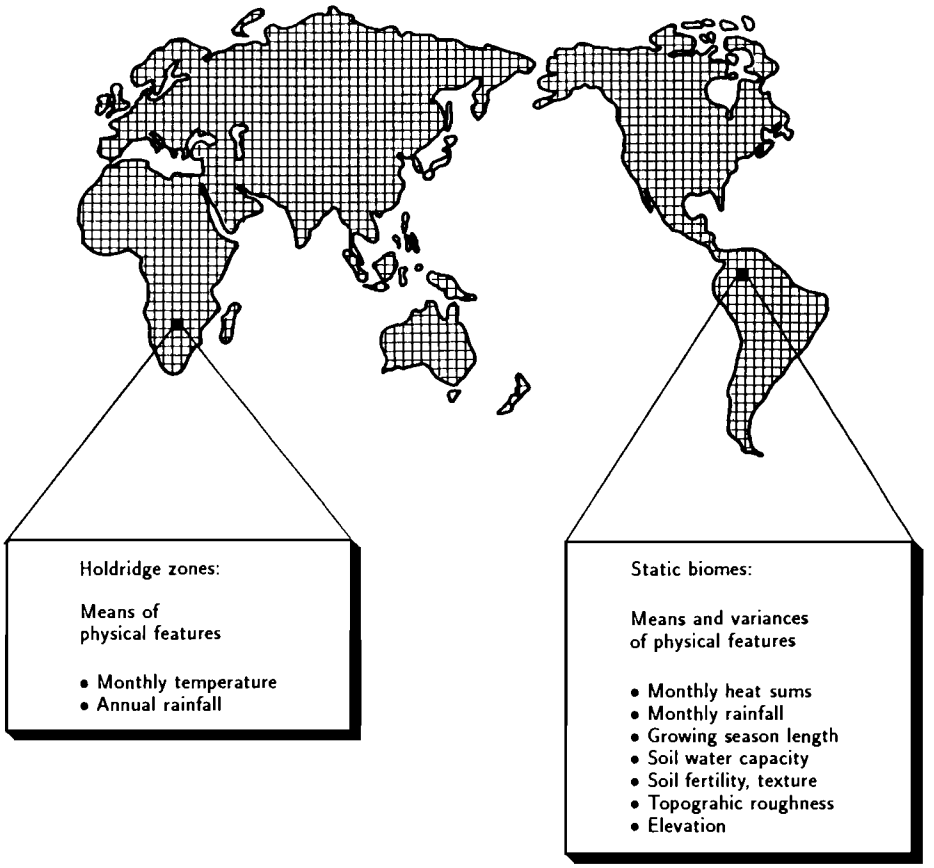

Figure 9. Static Grid Models: Holdridge system computerized by Emanuel *et al.* (1985) at left; improved data types being tested, at right.

Estimates of agro-ecological potential were obtained for specific areas by combining soil and climatic information. This approach is being expanded at IIASA to define the potential shifts in the crop-portion of global vegetation change. The soil and climatic requirements of 24 major crops (covering about 90% of the annual crop area in the developing countries) were identified using crop growth models. The environmental characteristics of specific areas were then matched with the requirements of individual crops in order to estimate the extent of land suitable for their production. The results of the AEZ Project were refined in the Land Resources for Future Populations (LRFP) Project of the Food and Agriculture Program at IIASA (FAO-UNFPA, 1980; Shah *et al.*, 1985). Extensions of the system, with more detail and including country-specific features, have

been applied to some individual countries, including Canada, Kenya, and Bangladesh.

These FAO studies provide a basis for predicting crop growth potentials as a function of changing climate. The following extensions are being undertaken:

- Since the AEZ and LRFP studies covered only the developing world (excluding China), the soil productivity and land-use constraints and estimates of agro-ecological potential must be assessed for the temperate-zone industrialized countries and China.
- Growing season length needs to be recalculated on a global basis, taking into account differences in the hydrological properties of soils. The surface hydrology model outlined above provides an approach to this problem.
- Some new crops must be included. Fourteen of the 24 crops for which there are AEZ growth models are important in the temperate zone and account for 65% of the total annually cropped area there, but the addition of a further eight crops would increase the coverage to 89%. This task may be fairly easy, if earlier classifications can be adapted. The Kenyan study had a growth model for sunflower, and the Canadian study gives climate and soil requirements for rape, sunflower, wine grape, rye, oats, clover, and sugar beet.
- Grassland production in the FAO models is tied to the length of the growing season without consideration of differences in soil moisture storage. Again, the surface hydrology model described above may provide a more mechanistic alternative to this analysis.

With sufficient global data and a system for their management and analysis, the AEZ methodology could be a powerful tool in the analysis of potential agricultural futures. For example, it offers analytical procedures for dealing with technological levels in relation to suitability ratings of land for specific crops. The methodology also offers analytical procedures with respect to soil degradation, mainly soil erosion. Yield loss functions developed in the FAO work could be used in estimating potential soil changes with changed climate and could help quantify some of the consequences for agricultural yields of soil degradation processes caused or enhanced by climatic change.

6. Global Data Management and Analysis

6.1. Large-scale vegetation studies

Continental-scale simulations of vegetation dynamics can be generated by deriving very large sets of patch model solutions. The region of interest, which may be the entire globe, is subdivided into landscape units on the order of 50 $\times$ 50 km each. A set of patch model solutions is generated for each of these landscape units, with appropriately distributed random environmental variables. Disturbance frequency and intensity are also specified; these may depend on environmental characteristics such as temperature or soil moisture as well as the status of vegetation.

The computer implementation of this Monte Carlo scheme for analyzing large-scale vegetation responses requires extensive geographic data management and analysis capabilities. Some features are needed that may not be important in smaller-scale applications:

- Values of some environmental variables, such as temperature and rainfall, must be estimated for each landscape unit by interpolating observations that usually have coarser spatial resolution. Others, such as topographic values, are available at much finer resolution. These higher-resolution topographic data sets can be used to provide indirect information on environmental variability within the landscape unit.
- Statistical analysis of available spatial data on landscape units is required, in order to help define relationships between topographic and environmental variability.
- Simulation results should be summarized as time series of *emergent* variables such as mean and variance of biomass, leaf-area index or species composition in each landscape unit. These results must be displayed as a sequence of maps. Video movies may be useful for visualization of map sequences.

In the following paragraphs, we describe geographic information systems that can be applied to global vegetation modeling and environmental data sets and that are sufficient for first tests of the Monte Carlo approach to global simulations.

6.2. Geographic information systems

Geographic information systems (GIS) combine graphics work stations, storage units, plotting devices, digitizing units with software for data input and verification, management and transformation, output, and presentation, to form an interactive user environment. Currently available systems do not meet all of the needs of global vegetation modeling efforts.

One approach to extending capabilities is to work with a GIS that is distributed with its source code programs. The Geographical Resources Analyses Support System (GRASS) is a general-purpose interactive geographic modeling and analysis package developed by USA-CERL-EN, a unit of the US Army Corps of Engineering. GRASS is written in the C programming language for the UNIX operating system. It provides tools for obtaining site information, digitizing existing maps, analyzing grid-cell data, analyzing neighborhood relations, generating map overlays based on different descriptive categories, generating slope and aspects maps, and displaying and scaling maps.

GRASS is grid cell oriented – it represents land surfaces as continuous arrays of rectangles. Each rectangle is assigned an integer value for variables such as vegetation type, soil type, or temperature and precipitation classes. Each variable is maintained as a separate grid data set – GRASS can overlay these for analysis. Arrays of point coordinates can be managed in GRASS to describe boundaries or to indicate point or linear features. The program requires

an experienced operator and is particularly applicable to the needs of computer programmers. Certain features limit our use of GRASS. The most important problem is the weak data input routines; the compatibility and interchangeability of data sets we require for cooperative work is poor at best. The projection system (equal area-equal distance) is also difficult to translate into latitude/longitude measures which we use.

IDRISI is a grid-based GIS, designed to give casual and first-time users access to inexpensive PC-based GIS technology (Eastman, 1988). IDRISI consists of independent modules for data entry, data conversion, data storage, data display, and several analytical tools. The modules are all linked by a simple data structure, which allows users to develop modules for their own purposes in program languages like FORTRAN or PASCAL. Although it contains too few data manipulation features for our project needs, the system is quite useful for short-term tasks and simple data inspections.

Arc/Info is an advanced polygon-based GIS, which can be installed under a wide variety of operating systems. It is more experience-requiring than is IDRISI, and less so than GRASS. It consists of a relational database and modules for map creation, map overlay and analysis, data conversion between different polygon and grid formats, and map display. Arc/Info is capable of importing data from many different sources. A macro-language is available to automate tasks which are used frequently. We are considering obtaining this system to fill the gap between the user-friendly IDRISI and the programmer's tool, GRASS.

Several data bases have been collected, error checked, and run at IIASA. These include the following.

6.3. Climatic data

- *World Weather Records* (Weather Bureau, 1959). Monthly average temperature and precipitation recorded at 2,583 meteorological stations worldwide.
- *Digitized World Climate Atlas* (Walter and Lieth, 1960). Monthly average temperature and precipitation values for 6,720 stations digitized from climate diagrams. Longitude, latitude, elevation, and the number of years of observation are given for each station.
- *Selected Global Climatic Data for Vegetation Science* (Müller, 1982). Climatic data selected from a collection of 1,048 meteorological stations. Monthly values are given for mean temperature, mean daily maximum and minimum temperature, absolute maximum and minimum temperature, mean relative humidity, mean precipitation, minimum and maximum precipitation, maximum precipitation in 24 hours, days with more than 0.1 mm precipitation, sunshine duration, global radiation, calculated potential evapotranspiration, and mean wind velocity and direction. There are missing values; maximum and minimum precipitation data are sparse.
- *Selected Weather Records for the USSR.* Monthly average temperature, humidity, first and last frost day, and monthly total precipitation for 1,074

stations throughout the USSR. The observation period is 1881–1965 for most stations. The data are distributed by the Institute for Hydro-Meteorological Information, Obninsk, USSR.

- *Northern Hemisphere Precipitation and Temperature Data* (Bradley *et al.*, 1985 and 1987). Long-term climatic data for Northern Hemisphere land areas, consisting of yearly and seasonal time series transformed onto a grid.
- *Simulated Climate* (Mitchell, 1983). Model experiments using the UK Meteorological Office general circulation model [(3° × 3°) spatial resolution]. Model output is available in the form of monthly averages from 3 years of simulated values of surface pressure, temperature, humidity, precipitation, and soil moisture. These are summarized for a reference case and with atmospheric CO_2 concentration at twice and four-times the reference value.

6.4. Related geographic data

- *FAO Soils Maps* (FAO/UNESCO, 1974). The 1:5,000,000 world soils maps consist of 26 major soil units and their subdivisions (106 total types). In addition, three textural, three slope, and twelve phase classes are distinguished.
  - (a) A 0.5° grid version, digitized by the University of New Hampshire. Grid cells are assigned a single soil type, phase, slope, and texture type if this could be determined unambiguously. Otherwise composite classes are used in grid cells.
  - (b) A 2 minute grid version, digitized by UNEP's GRID Project. The resolution of this version is so high that each cell is assigned unambiguously one of the soil classes. No information on texture, slope or phase is available in this data set.
- *Global Elevation Data.* Global elevation and topography data at a resolution of 10′ × 10′, assembled by the US Navy Fleet Numerical Oceanography Center at Monterey, California. Minimum, maximum and modal elevation; data on major ridges (number and orientation); terrain characteristics (salt or lake bed, flat, desert, ice, marsh, lake country, valley, ridge hills, average mountains, rugged mountains, ocean); fraction of water surface; and percentage of urban development are summarized.
- *Continental and National Boundaries.* Line-images of the coastlines, lakes and rivers, and international boundaries, with highest resolution for North America.
- *Major World Ecosystems Complexes* (Olson *et al.*, 1982). A 0.5° grid map of the world's major ecosystem complexes.
- *Holdridge Life Zones* (Emanuel *et al.*, 1985). A 0.5° world grid map of the Holdridge Life-Zone Classification (Holdridge, 1947).
- *World Vegetation Map* (Matthews, 1983). A 1° world grid map with 32 natural vegetation types, based on the UNESCO (1973) classification system.

- *World Cultivation Intensity Map* (Matthews, 1983). A 1° world grid map with 5 percentage classes of cultivation intensity.
- *World Albedo Map* (Matthews, 1983). A 1° world grid map with surface albedo classes for each season. This map is used on snow-free conditions, natural vegetation and cultivation characteristics.

7. Conclusion

This report describes progress during 1988 in developing models of global vegetation dynamics. The major modeling approach is to generate large numbers of solutions to a general model that describes vegetation growth on a small patch. The solutions sample the spatial distributions of environmental variables among patches within larger landscape units, for which mean values of environmental variables can be interpolated using existing global environmental data bases. This two-tier, Monte Carlo approach provides a convenient (if computationally demanding) way to link vegetation processes, many of which are small scale, to the global scale of atmospheric processes and available environmental data; it also provides a consistent way to build in disturbance regimes and mass effects.

We have described the specific topics and problems that are being addressed to develop a global vegetation analysis capability. The various model sections are not yet integrated – that integration is part of the model development and data assembly process, expected to progress greatly during the summer 1989 Model Workshop at IIASA. Summaries of several broad issues that current work is addressing follow.

General vegetation growth models. Individual-based forest models can be used in a Monte Carlo scheme to simulate large-scale vegetation change, but more concise, population-based models appear satisfactory – their organization is conducive to treating nonwoody plants and they require much less computing resource for solution. A central problem in finalizing the population based model we propose is to verify that the discrete height layers control leaf area advancement to the canopy with sufficient precision.

Given the assumption of horizontal homogeneity, the patch size is critical. It should correspond to the approximate area over which resources are shared so that plants compete. In many forests this area corresponds to the maximum size one or a few individuals. The death of an individual can then significantly influence the vertical light profile and allow gap-phase dynamics. Maximum crown sizes are smaller in boreal forests, and the patch size is possibly larger. In short-stature vegetation (i.e., heathlands) the patch size is much smaller (Prentice *et al.*, 1987). A scheme for varying spatial resolution is required to simulate gap dynamics in mixed life-form systems such as savannas (Smith and Urban, 1988).

In some patch models, competition for below-ground resources (water and nutrients) is not explicit; however, the population models can be extended to include this competition without changing their basic structure. This extension may be necessary to simulate competition when water and/or nutrients are

limiting, especially where there is competition between life forms with different rooting depths.

Functional plant types. The number of species that might be treated in global vegetation models is overwhelming – data to estimate parameters are not available for many species. More work needs to be done to systematize the cross-classification of plants into functional types for dynamic modeling and to specify valid response functions that modify growth increment according to water and nutrient availability, summer warmth, and winter cold.

Soils. We began developing a global vegetation model without explicitly treating soil dynamics. At this point, soil characteristics that influence vegetation are assumed fixed, but the tight interactions between vegetation and soils are not being ignored. Constant soils-related parameters can eventually be variables derived from soils modules. Organic matter changes, nutrient and water use, and even vegetation influences on physical processes affecting soils can be embedded in our model's vegetation description.

The cycles of major elements, including carbon, nitrogen, and phosphorus, can be simulated by linking compartment models to the vegetation patch description – empirical relationships between decomposition rates and litter quality can be used until appropriate general decomposition models are developed (Pastor and Post, 1986).

We need to identify models of soil genesis and long-term soil responses to climatic change that can be incorporated into the framework we are developing. Completion of this task will allow us to assess the consequences of climate changes at locations where major soils development will occur at rates similar to those of vegetation response.

Long-term direction of the modeling enterprise. Having adopted a Monte Carlo approach to simulating global vegetation dynamics, we face a difficult challenge in organizing and interpreting the solution set produced by any single exercise of such a model. Logistical tasks such as reorganization of simulation results to map plant functional type distributions or biomass variations are being accomplished as we extend geographical information systems to support global modeling activities. But the global science issues we want to address require conceptual developments as well. We must understand, *a priori*, which processes lead to species replacement sequences, determine boundaries between major vegetation types, and define the interactions between vegetation and other earth systems. These must then be modeled and be reflected in the large solution sets this model will produce. The effort by ourselves and others to characterize these processes will take many years, even with a highly successful and well-organized IGBP. However, the result will be to clarify the mechanisms through which vegetation will respond to global environmental change and the strategies useful in managing those changes or adapting to them.

References

Anonymous. 1984. *Atlas of the USSR.* Department for Geodesi and Cartography, Moscow.

Antonovsky, M.Ya. and M.D. Korzukhin. 1986. *Predictive Forest Ecosystem Models and Implications for Integrated Monitoring.* WP-86-36. International Institute for Applied Systems Analysis, Laxenburg, Austria.

Antonovsky, M.Ya., F.Z. Glebov, and M.D. Korzukhin. 1987a. *A Regional Model of Long-Term Wetland-Forest Dynamics.* WP-87-63. International Institute for Applied Systems Analysis, Laxenburg, Austria.

Antonovsky, M.Ya. and M.T. Ter-Mikhaelian. 1987b. *On Spatial Modelling of Long-Term Forest Fire Dynamics.* WP-87-105. International Institute for Applied Systems Analysis, Laxenburg, Austria.

Antonovsky, M.Ya., P.A. Kolosov, and A.A. Minin. 1988. *The Influence of the Underlying Land Surface on the Water Exchange Between Earth and Atmosphere.* WP-88-108. International Institute for Applied Systems Analysis, Laxenburg, Austria.

Bazzaz, F.A. 1979. The Physiological Ecology of Plant Succession. *Annual Review of Ecology and Systematics* **10**: 351–371.

Berliand, M.E. 1985. *Prediction and Regulation of Air Pollution.* Gidrometeoizdat, Leningrad [in Russian].

Bolin, B. 1984. Biogeochemical Processes and Climate Modelling. Pages 213–223 in J.T. Houghton (ed.) *The Global Climate.* Cambridge University Press, Cambridge, UK.

Bonan, G.B. 1988a. *Environmental Processes And Vegetation Patterns In Boreal Forests.* Ph.D. Dissertation. University of Virginia, Charlottesville, VA, USA.

Bonan, G.B. 1988b. *A Simulation Model of Environmental Processes and Vegetation Patterns in Boreal Forests: Test Case Fairbanks, Alaska.* WP-88-63. International Institute for Applied Systems Analysis, Laxenburg, Austria.

Bonan, G.B. and M.D. Korzukhin. 1989. Moss and Forest Interactions along a Soil Moisture and Soil Temperature Gradient in the Taiga of Interior Alaska. *Vegetatio* (submitted).

Bonan, G.B. and H.H. Shugart. 1989. Environmental Factors and Ecological Processes in Boreal Forests. *Annual Review of Ecology and Systematics* (in press).

Botkin, D.B., J.F. Janak, and J.R. Wallis. 1972. Some Ecological Consequences of a Computer Model of Forest Growth. *Journal of Ecology* **60**: 849–873.

Box, E.O. 1981. *Macroclimate and Plant Forms: An Introduction to Predictive Modeling in Phytogeography.* Dr.W. Junk Publ., Berlin, Germany, F.R.

Box, E.O. 1989. Estimating the Seasonal Carbon Source-Sink Geography of a Natural, Steady-State Terrestrial Biosphere. *Journal of Climate and Applied Meteorology* (in press).

Bradley, R.S., P.M. Kelly, P.D. Jones, C.M. Goodess, and H.F. Diaz. 1985. *A Climatic Databank for the Northern Hemisphere Land Areas, 1851–1980.* TR-017. Carbon Dioxide Research Division, US Department of Energy, Washington, DC, USA.

Bradley, R.S., H.F. Diaz, J.K. Eischeid, P.D. Jones, P.M. Kelly, and C.M. Goodess. 1987. Precipitation Fluctuations over the Northern Hemisphere Land Areas since the Mid-19th Century. *Science* **237**: 171–175.

Bristow, A. and B.Campbell. 1982. On the Relationship between Incoming Solar Radiation and the Daily Maximum and Minimum Temperature. *Agriculture and Forest Meteorology* **31**: 159–166.

Chapin, F.S. 1980. The Mineral Nutrition of Wild Plants. *Annual Review of Ecology and Systematics* **11**: 233–260.

Chapin, F.S., P.M. Vitousek, and K. Van Cleve. 1986. The nature of nutrient limitation in plant communities. *American Naturalist* **127**: 48–58.

Clark, W.C. 1986. Sustainable Development of the Biosphere: Themes for a Research Program. Pages 5–48 in W.C. Clark and R.E. Munn (eds.) *Sustainable Development of the Biosphere.* Cambridge University Press, Cambridge, UK.

Cramer, W.and I.C. Prentice. 1988. Simulation of Regional Soil Moisture Deficits on a European Scale. *Norsk Geografisk Tidsskrift* **42**: 149–151.

Dickinson, R.E. 1984. Modeling Evapotranspiration for Three-Dimensional Global Climate Models. Pages 58–72 in J.E. Hansen and T. Takahashi (eds.) *Climate Processes and Climate Sensitivity.* Geophysical Monographs 29. American Geophysical Union, Washington, DC, USA.

Doury, A. 1976. *Une Méthode de Calcul Pratique et General pour la Prévision Numerique des Pollutions Veniculeer par l'Atmosphère.* Report CEA-R-4280 (Rev.1). Centre d'Études Nucléaires de Seclay, Commissariat à l'Énergie Atomique, Paris, France.

Eagleson, P.S. 1978. Climate, Soil, and Vegetation. 4. The expected Value of Annual Evapotranspiration. *Water Resources Research* **14**: 731–739.

Eastman, J.R. 1988. *Idrisi. A Grid-Based Geographic Analysis System, Version 3.0.* Graduate School of Geography, Clark University, Worcester, MA, USA.

Ellenberg, H. 1954. Über einige Fortschritte der kausalen Vegetationskunde. *Vegetatio* **5/6**: 199–211.

Emanuel, W.R., H.H. Shugart, and M.P. Stevenson. 1985. Climatic Change and the Broad-Scale Distribution of Terrestrial Ecosystem Complexes. *Climatic Change* **7**: 29–43.

FAO. 1981. *Report on the Agro-Ecological Zones Project: Methodology and Results for Africa, Asia, and South and Central America.* World Soil Resources Report No. 48, Vols. 1–4. Food and Agriculture Organization, Rome, Italy.

FAO-UNFPA. 1980. *Report on the Second FAO/UNFPA Expert Consultation on Land Resources for Future Populations.* Rome, Italy.

FAO/UNESCO. 1974. *Soil Map of the World, 1:5,000,000.* Food and Agriculture Organization, Paris, France.

Federer, C.A. 1982. Transpiration Supply and Demand: Plant, soil, and Atmospheric Effects Evaluated by Simulation. *Water Resources Research* **18**(2): 355–362.

Fedorov, V.V. and S.E. Pitovranov. 1988. *Model Fitting and Optimal Design of Atmospheric Tracer Experiment. Part 1.* WP-88-65. International Institute for Applied Systems Analysis, Laxenburg, Austria.

Fowells, H.A. 1965. *Silvics of Forest Trees of the United States.* Agricultural Handbook No. 271. USDA Forest Service, Washington, DC, USA.

Grime, J.P. 1977. Evidence for the Existence of Three Primary Strategies in Plants and its Relevance to Ecological and Evolutionary Theory. *American Naturalist* **111**: 1169–1194.

Gurtsev, A.U. and M.D. Korzukhin. 1989. Crown and Root Competition in a One-Dimensional Pine Stand. In *Problems of Ecological Monitoring and Ecosystems Modelling*. Volume 11. Hydrometeoizdat, Leningrad, USSR (in press).

Haines, D.A., W.A. Main, J.S. Rost, and A.J. Simard. 1983. Fire-Danger Rating and Wildfire Occurrence in the Northeastern United States. *Forest Science* **29**: 679–696.

Heinselman, M.L. 1973. Fire in the Virgin Forests of the Boundary Waters Canoe Area, Minnesota. *Quaternary Research* **3**: 329–382.

Helmisaari, H.O. and N.T. Nikolov. 1989. *A Survey of Ecological Characteristics of Boreal Tree Species in Fennoscandia and USSR*. International Institute for Applied Systems Analysis, Laxenburg, Austria (forthcoming).

Hilmi, G.F. 1957. *Theoretical Biogeophysics of Forests*. AN, Moscow, USSR.

Holdridge, L.R. 1947. Determination of World Plant Formations from Simple Climatic Data. *Science* **105**: 367–368.

Horst, T.W. 1977. A Surface Depletion Model for Deposition from a Gaussian Plume. *Atmospheric Environment* **11**: 41–46.

Horovitz, C.C. and D.W. Schemske. 1986. Seed Dispersal and Environmental Heterogeneity in a Neotropical Herb: A Model of Population and Patch Dynamics. Pages 169–186 in A. Estrada and T.H. Fleming (eds.) *Frugivores and Seed Dispersal*. Junk, The Hague, Netherlands.

Huston, M.and T.M. Smith. 1987. Plant Succession: Life History and Competition. *American Naturalist* **130**: 168–198.

IAEA. 1986. *Atmospheric Dispersion Models for Application in Relation to Radionuclide Releases*. International Atomic Energy Agency, Vienna, Austria.

Jarvis, P.G. and J.W. Leverenz. 1983. Productivity of Temperate, Deciduous and Evergreen Forests. Pages 233–280 in O.L. Lange, P.S. Nobel, C.B. Osmond, and H. Ziegler (eds.) *Encyclopedia of Plant Physiology*. Vol. 12D. Springer-Verlag, Berlin, Germany, F.R.

Kataeva, K.V. and M.D. Korzukhin. 1987. *Dynamics of Dark-Coniferous-Cedar Forests*. Laboratory of Monitoring of Natural Environment and Climate, USSR State Committee of Hydrometeorology/Academy of Science, Moscow, USSR.

Kercher, J.R. and M.C. Axelrod. 1984. A Process Model of Fire Ecology and Succession in a Mixed-Conifer Forest. *Ecology* **65**: 1725–1742.

Korzukhin, M.D. and M.T. Ter-Mikhaelian. 1982. Competition for Light and Dynamics of Model Individuals Independently Distributed on the Plane. In *Problems of Ecological Monitoring and Ecosystems Modelling*. Volume 5. Hydrometeoizdat, Leningrad, USSR.

Korzukhin, M.D., V.N. Sedyh, and M.T. Ter-Mikhaelian. 1987. Formulation of a Prediction Model of Forest Regeneration-Age Dynamics. *Transactions of Academy of Science* Biological Series 20: 58–67.

Korzukhin, M.D., V.N. Sedyh, and M.T. Ter-Mikhaelian. 1989a. Application of a Prediction Model of Forest Regeneration-Age Dynamics to the *Pinus sibirica* Forests of the Middle Ob Region. *Transactions of Academy of Science* Biological Series (in press).

Korzukhin, M.D., G.B. Bonan, A.E. Rubina, M.Ya. Antonovsky, and A.M. Solomon. 1989b. *The Silvics of Some East European and Siberian Boreal Forest Tree Species*. International Institute for Applied Systems Analysis, Laxenburg, Austria (forthcoming).

Larcher, W. 1983. *Physiological Plant Ecology*. Springer-Verlag, New York, NY, USA.

Leemans, R.and I.C. Prentice. 1987. Description and Simulation of Tree-Layer Composition and Size Distributions in a Primaeval *Picea-Pinus* Forest. *Vegetatio* **69**: 147–156.

Leemans, R.and I.C. Prentice. 1989. FORSKA: A General Forest Succession Model. *Meddelanden från Växtbiologiska Institutionen.* Institute of Ecological Botany, Uppsala, Sweden (in press).

Lieth, H.and E.O. Box. 1972. Evapotranspiration and Primary Productivity: C.W. Thornthwaite Memorial Model. *Publications in Climatology* **25**: 37–46. Elmer, NJ, USA.

Linacre, E.T. 1968. Estimating the Net-Radiation Flux. *Agricultural Meteorology* **5**: 49–63.

Matthews, E. 1983. Global Vegetation and Land Use: New High-Resolution Data Bases for Climate Studies. *Journal of Climate and Applied Meteorology 22*: 474–487.

Miller, D.H. 1981. *Energy at the Surface of the Earth.* Academic Press, New York, NY, USA.

Mitchell, J.F.B. 1983. The Seasonal Response of a General Circulation Model to Changes in CO_2 and Sea Temperatures. *Quarterly Journal of the Royal Meteorological Society 109*: 113–152.

Müller, M.J. 1982. *Selected Climatic Data For A Global Set of Standard Stations for Global Vegetation Science.* Junk, The Hague, Netherlands.

Olejnik, J. 1988. *Present and Future Estimates of Evapotranspiration and Runoff for Europe.* WP-88-37. International Institute for Applied Systems Analysis, Laxenburg, Austria.

Olson, J.S., J.A. Watts, and L.J. Allison. 1982. *Carbon in Live Vegetation of Major World Ecosystems.* ORNL-5862. Oak Ridge National Laboratory, Oak Ridge, TN, USA.

Orians, G.H. and O.T. Solbrig. 1977. A Cost-Income Model of Leaves and Roots with Special Reference to Arid and Semi-Arid Areas. *American Naturalist* **111**: 677–690.

Parsons, R.F. 1968. The Significance of Growth Rate Comparisons for Plant Ecology. *American Naturalist* **102**: 295–297.

Pastor, J.and W.M. Post. 1986. Influence of Climate, Soil Moisture, and Succession on Forest Carbon and Nitrogen Cycles. *Biogeochemistry 2*: 3–27.

Prentice, I.C. 1986. Vegetation Responses to Past Climatic Variation. *Vegetatio* **67**: 131–141.

Prentice, I.C. 1989. Forest Dynamics and Climatic Change. In D.C. Glenn-Lewin (ed.) *Succession.* Chapman and Hall, London, UK.

Prentice, I.C., O. van Tongeren, and J.T. de Smidt. 1987. Simulation of Heathland Vegetation Dynamics. *Journal of Ecology* **75**: 203–219.

Prescott, J.A. 1940. Evaporation from a Water Surface in Relation to Solar Radiation. *Transactions of the Royal Society of Southern Australia* **64**: 114–125.

Rabinowitz, D.and J.K. Rapp. 1981. Dispersal Abilities of Seven Sparse and Common Grasses from a Missouri Prairie. *American Journal of Botany* **68**: 616–624.

Rodriguez, D.J. and L.C. Rosen. 1984. *An Evaluation of a Series of SF_6 Tracer Releases Using the MATHEW/ADDIC Model.* Report UCRL-91854. Lawrence Livermore National Laboratory, Livermore, California.

Rudakov, V.E. 1977. Can Judge about Transpiration of Forest for Its Productivity? *Isvestiya* VGO 109: 169–173.

Runkle, J.R. 1981. Gap Regeneration in Some Old-Growth Forests of the Eastern United States. *Ecology* **62**: 1041–1051.

Sellers, P.J., Y. Mintz, Y.C. Sud, and A. Dalcher. 1986. A Simple Biosphere Model (SiB) for Use within General Circulation Models. *Journal of the Atmospheric Sciences* **43**: 505–531.

Shah, M.M., G.M. Higgins, A.H. Kassam, and G. Fischer. 1985. *Land Resources and Productivity Potential – Agro-Ecological Methodology for Agricultural Development Planning.* CP-85-14. International Institute for Applied Systems Analysis, Laxenburg, Austria.

Shugart, H.H. 1984. *A Theory of Forest Dynamics.* Springer-Verlag, New York, NY, USA.

Shugart, H.H. and I.R. Noble. 1981. A Computer Model of Succession and Fire Response of the High Altitude *Eucalyptus* Forest of the Brindabella Range, Australian Capital Territory. *Australian Journal of Ecology* **6**: 149–164.

Smith, T.M. and M.P. Austin. 1989. Niche Pattern and the Distribution of Plants along Environmental Gradients. Manuscript in review.

Smith, T.M. and D.L. Urban. 1988. Scale and Resolution of Forest Structural Pattern. *Vegetatio* **74**: 143–150.

Solomon, A.M. 1986. Transient Response of Forests to CO_2-Induced Climate Change: Simulation Modeling Experiments in Eastern North America. *Oecologia* **68**: 567–579.

Solomon, A.M. and J.B. Harrington, Jr. 1979. Palynology Models. Pages 338–361 in R.L. Edmonds (ed.) *Aerobiology: The Ecological Systems Approach.* Dowden, Hutchinson, and Ross Publ., Stroudsburg, PA, USA.

Specht, R.L. 1972. Water Use by Perennial Evergreen Plant Communities in Australia and Papua New Guinea. *Australian Journal of Botany* **20**: 273–299.

Specht, R.L. 1981. Growth Indices – Their Role in Understanding the Growth, Structure and Distribution of Australian Vegetation. *Oecologia* **50**: 347–356.

Swift, L.W., Jr. 1976. Algorithm for Solar Radiation on Mountain Slopes. *Water Resources Research* **12**: 108–112.

Ter-Mikhaelian, M.T. and V.V. Furyaev. 1988. Spatial Model of Long-Term Forest Dynamics Taking into Account Influence of Wildfires. In *Problems of Ecological Monitoring and Ecosystems Modelling.* Vol.11. Hydrometeoizdat, Leningrad, USSR (in press).

Tilman, D. 1988. *Plant Strategies and the Dynamics and Structure of Plant Communities.* Monograph in Plant Biology, 26. Princeton University Press, Princeton, NJ, USA.

UNESCO. 1973. *International Classification and Mapping of Vegetation.* UNESCO, Paris, France.

Van Cleve, K., L.Oliver, R. Schlentner, L.A. Viereck, and C.T. Dyrness. 1983. Productivity and Nutrient Cycling in Taiga Forest Ecosystems. *Canadian Journal of Forest Research* **13**: 747–766.

Vernadsky, W.I. 1945. The Biosphere and the Noosphere. *American Scientist* **33**: 1–12.

Walter, H. 1973. *Vegetation of The Earth.* Springer-Verlag, Heidelberg, Germany, F.R.

Walter, H. and H. Lieth. 1960. *Klimadiagramm – Weltatlas.* VEG Fisher-Verlag, Jena, Germany, D.R.

Waring, R. 1983. Growth Efficiency. *Advances in Ecological Research* **13**: 327–354.

Weather Bureau. 1959. *World Weather Records 1941–1950.* US Department of Commerce, Washington, DC, USA.

White, P.S. 1979. Pattern, Process, and Natural Disturbance in Vegetation. *Botanical Reviews* **45**: 229–299.

Woodward, F.I. 1987. *Climate and Plant Distribution.* Cambridge University Press, Cambridge, UK.

Contributors

Gordon B. Bonan, National Center for Atmospheric Research, PO Box 3000, Boulder, CO 80307-3000, USA.

William R. Emanuel, Environmental Sciences Division, Oak Ridge National Laboratory, Oak Ridge, TN 37831-6038, USA.

Sandy P. Harrison, Department of Physical Geography, Uppsala University, Box 554, S-75122 Uppsala, Sweden.

Harry O. Helmisaari, Department of Ecological Botany, Uppsala University, Box 559, S-75122 Uppsala, Sweden.

Janos P. Hrabovszky, Wienerbruckstraße 85/III, A-2344 Südstadt/Maria Enzersdorf, Austria.

Mikhail D. Korzukhin, Goskohydromet Natural Environment and Climate Monitoring Laboratory, 20B Glebovskaya St., 107258 Moscow, USSR.

Sandra Lavorel, Centre d'Études Phytosociologiques et Écologiques Louis Emberger, Centre National de la Recherche Scientifique, Route de Mende, BP 5051, F-34033 Montpellier Cedex, France.

Rik Leemans, Biosphere Project, International Institute for Applied Systems Analysis, A-2361 Laxenburg, Austria.

Alexander A. Minin, Goskohydromet Natural Environment and Climate Monitoring Laboratory, 20B Glebovskaya St., 107258 Moscow, USSR.

Nedialko T. Nikolov, Higher Institute for Forestry and Forest Technology, K. Ochridski 10, BG-1156 Sofia, Bulgaria.

Sergei E. Pitovranov, Institute for Systems Studies, 9, Prospect 60 Let Octyabria, 117312 Moscow, USSR.

I. Colin Prentice, Institute of Ecological Botany, Uppsala University, Box 559, S-75122 Uppsala, Sweden.

Thomas M. Smith, Department of Environmental Sciences, University of Virginia, Clark Hall, Charlottesville, VA 22903, USA.

Allen M. Solomon, Biosphere Project, International Institute for Applied Systems Analysis, A-2361 Laxenburg, Austria.

Mikhail T. Ter-Mikhaelian, Goskohydromet Natural Environment and Climate Monitoring Laboratory, 20B Glebovskaya St., 107258 Moscow, USSR.

Robert S. Webb, Department of Geological Sciences, Brown University, Providence, RI 02912-1846, USA.